



Published in final edited form as:

*Circulation*. 2023 July 04; 148(1): 47–67. doi:10.1161/CIRCULATIONAHA.123.063760.

## ***INKILN* is a novel long noncoding RNA promoting vascular smooth muscle inflammation via scaffolding MKL1 and USP10**

Wei Zhang, PhD<sup>1,\*,#</sup>, Jinjing Zhao, MD and PhD<sup>2,\*</sup>, Lin Deng, PhD<sup>3</sup>, Nestor Ishimwe, PhD<sup>1</sup>, Jessica Pauli, MSc<sup>4</sup>, Wen Wu, PhD<sup>2</sup>, Shengshuai Shan, MD and PhD<sup>1</sup>, Wolfgang Kempf, PhD<sup>4</sup>, Margaret D Ballantyne, PhD<sup>3</sup>, David Kim, BS<sup>1</sup>, Qing Lyu, PhD<sup>1</sup>, Matthew Bennett, PhD<sup>3</sup>, Julie Rodor, PhD<sup>3</sup>, Adam W. Turner, PhD<sup>5</sup>, Yao Wei Lu, PhD<sup>2</sup>, Ping Gao, PhD<sup>2</sup>, Mi Hyun Choi, PhD<sup>2</sup>, Ganesh Warthi, PhD<sup>1</sup>, Ha Won Kim, PhD<sup>1</sup>, Margarida M Barroso, PhD<sup>2</sup>, William B. Bryant, PhD<sup>1</sup>, Clint L. Miller, PhD<sup>5,6</sup>, Neal L. Weintraub, MD<sup>1</sup>, Lars Maegdefessel, MD, PhD<sup>4,7,8</sup>, Joseph M. Miano, PhD<sup>1</sup>, Andrew H Baker, PhD<sup>3</sup>, Xiaochun Long, PhD<sup>1,2,#</sup>

<sup>1</sup>Vascular Biology Center, Medical College of Georgia at Augusta University, Augusta, GA, USA

<sup>2</sup>Department of Molecular and Cellular Physiology, Albany Medical College, Albany, NY, USA

<sup>3</sup>Centre for Cardiovascular Science University of Edinburgh, Edinburgh, Scotland

<sup>4</sup>Department for Vascular and Endovascular Surgery, Klinikum rechts der Isar, Technical University Munich, Germany

<sup>5</sup>Center for Public Health Genomics, University of Virginia, Charlottesville, VA, USA

<sup>6</sup>Department of Biochemistry and Molecular Genetics, University of Virginia, Charlottesville, VA, USA

<sup>7</sup>German Center for Cardiovascular Research (DZHK, partner site Munich), Germany

<sup>8</sup>Department of Medicine, Karolinska Institute, Stockholm, Sweden

### **Abstract**

**Background:** Activation of vascular smooth muscle cell (VSMC) inflammation is vital to initiate vascular disease. However, the role of human-specific long noncoding RNAs (lncRNAs) in VSMC inflammation is poorly understood.

**Methods:** Bulk RNA-seq in differentiated human VSMCs revealed a novel human-specific lncRNA called Inflammatory MKL1 Interacting Long Noncoding RNA (*INKILN*). *INKILN*

#Correspondence: Wei Zhang, Ph.D., WZHANG1@augusta.edu; Xiaochun Long, Ph.D., Xlong@augusta.edu, Vascular Biology Center, Medical College of Georgia at Augusta University, 1460 Laney Walker Blvd, Augusta, GA. Tel: 706-446-0157.

\*These authors share equal authorship.

#### Author contributions

WZ, JZ, DL, MMB, and XL designed and performed the research. WZ, JZ, DL, WW, SS, NI, JP, WK, AWT, YWL, MDB, MB, JR, DK, QL, GW, PG, and MC performed experiments and analyzed the data. HWK, NLW, CM, AHB, and LM contributed to human sample studies. JMM, AHB, MMB and LM participated in research design and edited the manuscript. WZ and XL wrote the paper. The authors declare no conflicts of interest.

#### Disclosure

None

#### Conflicts of Interest

None

expression was assessed in multiple in vitro and ex vivo models of VSMC phenotypic modulation as well as human atherosclerosis and abdominal aortic aneurysm (AAA). The transcriptional regulation of *INKILN* was verified through luciferase reporter and chromatin immunoprecipitation assays. Loss- and gain-of-function studies and multiple RNA-protein and protein-protein interaction assays were utilized to uncover a mechanistic role of *INKILN* in the VSMC proinflammatory gene program. Bacterial Artificial Chromosome (BAC) transgenic (Tg) mice were used to study *INKILN* expression and function in ligation injury-induced neointimal formation.

**Results:** *INKILN* expression is downregulated in contractile VSMCs and induced in human atherosclerosis and AAA. *INKILN* is transcriptionally activated by the p65 pathway, partially through a predicted NF- $\kappa$ B site within its proximal promoter. *INKILN* activates proinflammatory gene expression in cultured human VSMCs and ex vivo cultured vessels. Mechanistically, *INKILN* physically interacts with and stabilizes MKL1, a key activator of VSMC inflammation through the p65/NF- $\kappa$ B pathway. *INKILN* depletion blocks IL1 $\beta$ -induced nuclear localization of both p65 and MKL1. Knockdown of *INKILN* abolishes the physical interaction between p65 and MKL1 and the luciferase activity of an NF- $\kappa$ B reporter. Further, *INKILN* knockdown enhances MKL1 ubiquitination, through reduced physical interaction with the deubiquitinating enzyme, USP10. *INKILN* is induced in injured carotid arteries and exacerbates ligation injury-induced neointimal formation in BAC Tg mice.

**Conclusions:** These findings elucidate an important pathway of VSMC inflammation involving an *INKILN*/MKL1/USP10 regulatory axis. Human BAC Tg mice offer a novel and physiologically relevant approach for investigating human-specific lncRNAs under vascular disease conditions.

### Keywords

long noncoding RNA; inflammation; vascular smooth muscle cell; ubiquitination; human BAC transgenic mice

### Introduction

Vascular homeostasis is maintained by the interplay of signaling pathways between resident and circulating cells. Humoral, physical, or mechanical perturbations to the vessel wall trigger inflammation.<sup>1</sup> Sustained and over-activated vascular inflammation leads to vascular cell maladaptation and pathological vascular remodeling.<sup>1</sup> Excessive vascular inflammation underlies virtually all pathological events in the vasculature, including neointimal formation, lipid accumulation, plaque destabilization, aortic rupture, and thrombosis.<sup>2</sup> Targeting vascular inflammation is considered a promising strategy to combat different vascular disorders as evidenced by numerous preclinical animal trials as well as the CANTOS Trial.<sup>3-7</sup> Despite these efforts, successful implementation of anti-inflammatory strategies for vascular diseases remains disappointing.<sup>8,9</sup> This is likely due to the challenges in selectively targeting vascular inflammation among the highly complex network of systemic inflammatory pathways. As such, a better understanding of the molecular underpinnings of vascular inflammation, particularly as to how diverse coding and noncoding genes intertwine to govern this process, is essential to develop effective anti-inflammatory based therapeutics for vascular disease.

The human genome undergoes pervasive transcription of long non-coding RNAs (lncRNAs), defined as processed transcripts of length > 200 nucleotides that do not encode for a stable protein.<sup>10, 11</sup> Unlike mRNAs, which are highly conserved across mammalian species, the majority of lncRNAs are human-specific, precluding loss-of-function studies in rodent models. Recent studies have identified numerous human-specific lncRNAs associated with complex cardiometabolic traits.<sup>12</sup> Characterization of these human-specific lncRNAs in cardiovascular pathophysiology remains challenging due to the lack of *in vivo* models. Engineering mice with BACs carrying human sequences, especially human lncRNA gene loci, represents a potentially effective approach to this endeavor.<sup>13, 14</sup> However, this strategy has yet to be harnessed for *in vivo* investigation of a lncRNA under a vascular disease context.

A number of lncRNAs have been documented as key regulators in various biological processes and human diseases.<sup>15</sup> The actions of lncRNAs depend on their cellular localization, which confers the physical accessibility to their interactive partners for function. Nuclear lncRNAs can modulate gene expression by associating with DNA, transcription factors, and epigenetic modifiers while cytosolic lncRNAs partner with diverse factors to influence protein translation, RNA or protein stability, and protein activity.<sup>16</sup> Recent efforts have revealed the important roles of lncRNAs in vascular pathophysiology, such as VSMC differentiation, angiogenesis, oxidative stress, senescence, endothelial permeability, and, more recently, endothelial to mesenchymal transition.<sup>17–22</sup> Several lncRNAs have been reported to regulate vascular inflammation. For example, the human-specific *lncRNA-CCL2* positively regulates its neighboring protein coding gene, *CCL2*.<sup>23</sup> *VINAS* promotes atherosclerosis via activating NF- $\kappa$ B and MAPK signaling pathways.<sup>24</sup> Hematopoietic *MALAT1* inhibits vascular inflammation through sponging microRNA miR-503.<sup>25</sup> While these studies and others have been conducted in endothelial cells and macrophages, lncRNA function in VSMC inflammation is poorly understood.<sup>19, 24</sup> Elucidating inflammatory lncRNAs in VSMC phenotype transition is of critical importance given the established role of VSMCs in such inflammatory vascular diseases as atherosclerosis and aneurysm formation.<sup>26</sup>

The widely expressed Myocardin related transcription factor A (MRTFA, MKL1) is a multifaceted transcription factor, initially recognized as a cofactor of SRF to facilitate CArG-dependent gene transcription of the VSMC contractile gene program.<sup>27, 28</sup> In contrast to MYOCD and MRTFB (MKL2), whose function is to establish and maintain VSMC differentiation,<sup>29</sup> MKL1 expression is robustly induced by and contributes to diverse vascular pathologies, including neointimal formation, atherosclerosis, hypertension, aortic dissection, and aneurysm.<sup>30–34</sup> The pathological role of MKL1 in the vasculature is mediated by disparate gene programs, including extracellular matrix, oxidative stress, and vascular inflammation.<sup>33, 34</sup> The proinflammatory action of MKL1 has been attributed to its crosstalk with the p65/NF- $\kappa$ B regulatory axis, either through physical interaction with p65 to transactivate proinflammatory genes, or complexing with epigenetic modifiers to confer an active chromatin state around proinflammatory genes.<sup>35, 36</sup> As such, it is of particular importance to understand how MKL1 is induced and stabilized under pathological conditions. However, the mechanisms underlying MKL1 expression in vascular disease contexts, particularly at the protein level, are virtually unknown.<sup>37</sup>

In the present study, unbiased RNA-seq revealed a novel human-specific lncRNA, called Inflammatory MKL1 Interacting Long Noncoding RNA or *INKILN*. We show that *INKILN* is positively associated with and activates a proinflammatory VSMC phenotype via a MKL1/p65 pathway. This involves *INKILN* physical interaction with MKL1 and a deubiquitinase, USP10, to prevent ubiquitin-dependent MKL1 degradation. Using a humanized *INKILN* transgenic mouse model, we demonstrate that *INKILN* is induced by and contributes to neointimal formation following carotid artery ligation. In addition to revealing a new lncRNA and molecular mechanism underlying the proinflammatory VSMC phenotype and vascular pathology, we present an innovative BAC transgenic (Tg) approach to study the *in vivo* regulation and function of human-specific lncRNAs in models of human disease.

## Methods

The bulk RNA-seq in HCASMCs overexpressing Myocardin (MYOCD) and data analysis were described previously and related data were deposited in the Gene Expression Omnibus (GEO) database (GSE77120).<sup>17</sup> Long-read sequence data for BAC Tg have been submitted to NCBI SRA database ([www.ncbi.nlm.nih.gov/sra](http://www.ncbi.nlm.nih.gov/sra)) under BioProject number PRJNA873299. Human sample studies were conducted in accordance with the related human subject study protocol, which was approved by the Institutional Review Board (IRB) at the Klinikum rechts der Isar of the Technical University Munich. All animal studies were approved by the Augusta University Animal Care and Use Committee. Detailed information on the related reagents and methods is provided in Supplemental Material. All other data that support the findings of this study are available from the corresponding authors upon reasonable request.

## Statistical analysis

All experiments were repeated in at least 3 independent experiments. Statistical analyses were conducted with GraphPad Prism 9.0. Quantitative results were presented as mean  $\pm$  standard deviation (SD). *In vivo* data with sample size  $> 10$  were first tested for normal distribution (Gaussian distribution) via D'Agostino-Pearson normality test. A t-test was used when the two groups were both normally distributed and a nonparametric Mann-Whitney test was used for groups having a non-Gaussian distribution. We used two-sample t-test when comparing two independent samples; paired t-test was used when required by the experimental design, as indicated in figure legends. The unpaired comparisons that did not have equal variances were analyzed by a t-test with Welch's correction. Comparisons for more than two groups with equal variances were conducted with one-way ANOVA. In case of unequal variances, Brown-Forsythe ANOVA test was used. If two groups were compared to the same control group, one-way ANOVA followed by a Dunnett's test was used. For all pairwise comparisons, one-way ANOVA followed by Bonferroni test was used (e.g., Figure 5D). Two-way ANOVA followed by a Tukey's post hoc test was used for multiple comparisons with two variances.  $p < 0.05$  was considered statistically significant. The detailed information for all the statistical analyses is included in Table S6.

## Results

### ***INKILN* expression correlates with VSMC phenotypic modulation and vascular disease**

In an effort to uncover novel lncRNAs linked to VSMC phenotypic modulation and vascular disease, we conducted a bulk RNA-seq analysis in human coronary artery smooth muscle cells (HCASMs) overexpressing MYOCD, a potent activator of VSMC differentiation. <sup>50</sup> Assembling the filtered reads derived from RNA sequencing to the human genome browser revealed numerous MYOCD-regulated protein coding genes (gray) and noncoding RNAs (red). Beyond a number of upregulated lncRNAs, such as *MYOSLID*, which we reported as an activator of VSMC differentiation, <sup>17</sup> MYOCD also downregulates many lncRNAs. *INKILN* appeared to be one of the most abundantly expressed, and significantly downregulated lncRNAs (Figure 1A). To determine cell and tissue-specific expression of *INKILN*, we employed FANTOM (Functional Annotation Of the Mammalian genome) expression atlas, a meta-annotation which integrates reference genes and newly defined transcription start sites (TSSs) based upon CAGE-seq. <sup>51</sup> Analysis of 173 cell types and 174 tissues in FANTOM revealed that *INKILN* was enriched in 5 different types of VSMCs, including SMC of the internal thoracic artery, SMC of the carotid artery, vascular associated SMC, aortic SMC, as well as different blood vessels which are enriched with VSMCs (Figure S1A). Consistently, quantitative RT-PCR (qRT-PCR) showed selective expression of *INKILN* in multiple HCASMC isolates, the human VSMC cell line, HITB5, SMC-like myofibroblasts (BR5), and Rhabdomyosarcoma (RD) cells, all of which express the VSMC contractile gene *LMOD1*, as we reported previously (Figure S1B). <sup>17</sup> qRT-PCR experiments confirmed downregulation of *INKILN* by MYOCD (Figure 1B). *INKILN* was also downregulated by TGF $\beta$ 1, another well-recognized activator of VSMC differentiation, <sup>52</sup> and a commercial source of conditioned VSMC differentiation medium (SMD); like *LMOD1*, the VSMC contractile gene, *CNN1*, was upregulated under these conditions (Figure 1C, 1D). Upon ex vivo organ or primary cell culture, VSMCs undergo dedifferentiation, resulting in the downregulation of VSMC contractile genes. <sup>53</sup> In contrast to the VSMC contractile gene *MYH11*, *INKILN* was undetectable in freshly obtained human saphenous veins (HSVs), whereas it was induced in ex vivo cultured HSV segments and primary HSVSMCs dispersed from the same vessel source (Figure 1E, 1F).

Because VSMC phenotypic modulation contributes to the pathogenesis of various vascular diseases, we asked if *INKILN* expression is induced in diseased vessels. We first analyzed the combined single nucleus (sn) ATAC libraries from healthy versus diseased coronaries, <sup>40</sup> and found three human atherosclerosis-associated peaks residing in intron 1 of *INKILN*. Interestingly, these peaks overlap with macrophage-specific peaks (Figure 1G). Further, qRT-PCR showed markedly elevated *INKILN* expression in atherosclerotic plaques compared to non-atherosclerotic regions from the same vessel source, and human AAA tissues versus normal aortas from healthy donors. As expected, gene expression of *CNN1* was downregulated in both atherosclerosis and AAA, which is in contrast to the proinflammatory gene *IL8* (Figure 1H, 1I). Immuno-RNA FISH showed a clear colocalization of *INKILN* with ACTA2 positive cells in the neointimal region of human AAA tissues, presumably representing phenotypically modulated VSMCs (Figure. 1J); a negative control probe failed to give rise to such signal (Figure S1C). Collectively, these

results demonstrate that *INKILN* is a VSMC-enriched lncRNA negatively associated with the VSMC contractile phenotype and induced in vascular disease.

### ***INKILN* is induced by proinflammatory stimuli through the NF- $\kappa$ B/p65-dependent pathway**

*INKILN* is an intergenic lncRNA residing on chromosome 4, 20 kilobases upstream of *IL8*. Two splice variants of *INKILN* were found according to sequence assembly, which we refer to as *V1* and *V2* (Figure S2A). RACE and sequencing demonstrated that the full length of *V1* and *V2* is 1,750 bp and 543 bp, respectively. Because of the much lower expression of *V2* (Figure S2B), we selected *V1* for overexpression experiments in this study. PhyloCSF analysis and Pfam database query support the absence of any coding potential of *INKILN* (Figure S2C). In vitro transcription/translation assay further validated the absence of protein coding potential in *INKILN* (Figure S2D).

To determine the critical pathway(s) responsible for the induction of *INKILN* in dedifferentiated VSMCs, we analyzed our published bulk RNA-seq dataset (GSE69637) done with HSVSMCs treated with proinflammatory cytokine IL1 $\alpha$  and PDGF, two critical stimuli driving VSMC dedifferentiation.<sup>54</sup> *INKILN* was induced by IL1 $\alpha$  but not PDGF, which was further confirmed by qRT-PCR, suggesting the proinflammatory, but not proliferative, pathway governs *INKILN* induction in VSMCs (Figure 2A, 2B). Dose-dependent studies in HSVSMCs showed that induction of *INKILN* expression was achieved by IL1 $\alpha$  with concentrations as low as 0.01 ng/ml (Figure S2E). Similar induction was seen in HCASMCs, human aortic SMCs (HASMCs), as well as pulmonary artery SMCs (PASMCs) using different proinflammatory cytokines, such as TNF $\alpha$  and IL1 $\beta$  (Figure 2C–F, Figure S2F). In HASMCs, IL1 $\beta$ -induced *INKILN* was time-dependent with peak elevation at 12 hours following treatment. This dynamic induction paralleled its neighboring gene, *IL8* (Figure 2G). IL1 $\beta$ -induced *INKILN* was suppressed by BAY11-7082, a selective inhibitor of the NF- $\kappa$ B pathway (Figure 2H). Overexpression of IKK $\beta$ , a specific activator of the NF- $\kappa$ B pathway, caused a significant induction of both *INKILN* and *IL8* (Figure 2I), suggesting an NF- $\kappa$ B -dependent induction of *INKILN* expression. To determine if *INKILN* was a direct transcriptional target of the NF- $\kappa$ B pathway, we conducted computational analysis of the proximal promoter of *INKILN* wherein a conserved NF- $\kappa$ B site was predicted (Figure S2A). Chromatin immunoprecipitation (ChIP) assays showed that IL1 $\beta$  induced p65 binding to the proximal promoter region encompassing a predicted NF- $\kappa$ B site in HASMCs (Figure 2J). Finally, TNF $\alpha$  significantly increased the luciferase activity of a reporter containing this NF- $\kappa$ B site, whereas such induction was diminished in a truncated version lacking this site (Figure 2K). These data support *INKILN* as a direct transcriptional target of the p65/NF- $\kappa$ B pathway.

### ***INKILN* positively regulates proinflammatory gene expression in VSMCs**

The massive induction of *INKILN* by proinflammatory stimuli suggests that *INKILN* participates in the proinflammatory gene program in VSMCs. To test this hypothesis, we performed RNA-seq in HASMCs treated with two different siRNAs, individually or in combination, to *INKILN* followed by IL1 $\beta$  or vehicle control treatment for 24 hours. Principal Component Analysis (PCA) revealed that samples from the same condition clustered together, and differences were evident between control and *INKILN* siRNA



treated groups under both vehicle and IL1 $\beta$  stimulated conditions (Figure S3A). We next performed differential expression analysis based on an adjusted p-value  $\leq 0.05$  for each set of raw expression measures. A total of 548 genes were significantly differentially expressed in si*INKILN* versus siCtrl under basal conditions, with 333 of them downregulated by si*INKILN*. Notably, of 838 significantly regulated genes under the IL1 $\beta$  stimulated condition, 518 were downregulated (see information in **GSE158219**). To identify the pathways regulated by *INKILN* and gain insight into *INKILN* molecular functions in VSMCs, we performed Gene Ontology (GO) enrichment analysis and KEGG pathway analysis. The majority of downregulated pathways upon si*INKILN* knockdown were associated with inflammation-related biological processes, including pathways of cellular response to cytokine stimulus, cytokine-mediated signaling, chemokine-mediated signaling, and positive regulation of MAPK cascade (Figure 3A). KEGG pathway analysis further identified several pathways related to inflammation and immune response such as TNF signaling, Cytokine-cytokine receptor interaction, IL-17 signaling, and NF- $\kappa$ B signaling (Figure S3B). Numerous proinflammatory genes, including those encoding chemokines and cytokines (*CXCL1*, *IL8*, and *IL6*), as well as other inflammatory mediators (*NR4A2*, *PTGS2*, and *OLR1*), were downregulated upon *INKILN* depletion under basal and IL1 $\beta$ -induced conditions (Figure 3B). Downregulation of proinflammatory genes, such as *IL8*, *IL6*, *CCL2*, and *CXCL1*, was validated by qRT-PCR in both basal and IL1 $\beta$ -induced HASMCs, growing HCASMCs, and TNF $\alpha$ -induced PASMCs (Figure 3C, 3D, Figure S3C). These results were further validated by a separate siRNA in HASMCs (Figure S3D). To independently confirm the siRNA results, we utilized FANA ASO, an alternative approach for gene knockdown based on RNase H-mediated RNA-degradation.<sup>55, 56</sup> FANA-mediated *INKILN* knockdown resulted in a similar downregulation of proinflammatory genes in both growing HASMCs and HCASMCs, though to a lesser degree compared with siRNA, likely due to lower knockdown efficiency (Figure 3E, 3F). In line with the results from loss-of-function studies, lentivirus overexpressing *INKILN* (Lenti-*INKILN*) induced *IL6*, *IL8*, *CXCL1*, and *CXCL5* gene expression in HASMCs (Figure 3G). To test if *INKILN* functions similarly in the human vasculature, we utilized a well-recognized organ culture model to recapitulate pathological vein remodeling in HSV bypass grafts.<sup>39</sup> Robust induction of most proinflammatory genes, including *INKILN*, *IL8*, *IL6*, and *CXCL5*, was observed in HSV segments cultured for 3 days (Figure S3E). Notably, siRNA was efficiently delivered to the vasculature, as evidenced by 70% *INKILN* knockdown in the cultured segments, leading to a significant reduction of *IL8*, *IL6*, and *CXCL5* gene expression (Figure 3H). Taken together, these results demonstrate that *INKILN* is a novel activator of the proinflammatory gene program in cultured VSMCs and ex vivo cultured vessels.

### ***INKILN* interacts with MKL1 in the cytoplasm of VSMCs**

To gain insight into the mechanism through which *INKILN* promotes inflammatory gene expression, we sought to determine its cellular localization in cultured VSMCs. qRT-PCR of total RNA from fractionated HCASMs showed that *INKILN* was distributed primarily in the cytosolic compartment (Figure 4A), a finding further confirmed by single molecule RNA-FISH (Figure 4B, **left**). The *INKILN* signal was authenticated by siRNA-mediated *INKILN* gene knockdown and a negative control probe (Figure 4B, **middle**; Figure S4A). Quantitation of *INKILN* positive cells revealed an average copy number of  $\sim 17$  *INKILN*

transcripts per cell (Figure 4B, **right**). Because of the robust induction of MKL1 protein levels, its established role in vascular inflammation and disease,<sup>34–36</sup> and its high RNA binding potential revealed by a well-recognized algorithm, CatRAPID (Figure S4B),<sup>57</sup> we sought to test if MKL1 could be an interactive partner of *INKILN*. In vitro RNA pull-down coupled with Western blotting revealed enriched interaction between MKL1 and the *INKILN* transcript, but not the negative control corresponding to antisense *INKILN* (Figure 4C). This interaction appeared to be specific, as two well-recognized activators of inflammation, p65 and p38, were not pulled down by *INKILN* (Figure S4C). Further, RNA immunoprecipitation (RIP)-qPCR showed a high enrichment of *INKILN* in the RNA precipitates pulled down by MKL1 antibody, but not p65 antibody and the negative control IgG in HCASMCs (Figure 4D) and human rhabdomyosarcoma (RD) cells (Figure 4E). This enrichment was specific to *INKILN* as two abundant transcripts, *18S* (Figure 4D) and *RNU6-1*, were not enriched by anti-MKL1 precipitation (Figure 4E). Immuno-RNA-FISH studies revealed *INKILN* and MKL1 protein mainly colocalize in the cytosol of HCASMCs (Figure 4F). Such cytosolic colocalization in VSMCs was specific to MKL1 as no colocalization was seen with ACTA2, a highly expressed cytoskeletal protein, and the species-matched negative control IgG (Figure 4F; Figure S4D). Pearson correlation coefficient analysis revealed a higher correlation score for MKL1 with *INKILN*, but not *PP1B* (Figure 4G). To further validate cytosolic colocalization between *INKILN* and MKL1, we stimulated the cells with Jasplakinolide (Jpk) and TGFβ1, two established activators of MKL1 nuclear translocation.<sup>58</sup> Though enhanced nuclear MKL1 was seen after stimulation by both activators, colocalization was retained in the cytosol (Figure 4H, **Left**). The correlation in colocalization between MKL1 and *INKILN* was reduced upon either Jpk or TGFβ1 treatment compared with their individual controls (Figure 4H, **Right**), likely attributable to the decreased amount of cytosolic MKL1 protein following nuclear translocation. These data support *INKILN* physically interacting with MKL1 in the cytosolic compartment of VSMCs.

### Loss of *INKILN* suppresses MKL1/p65-mediated activation of the proinflammatory gene program

The transcription factor MKL1 functions as a critical activator of inflammation in both cultured VSMCs and vascular disease models.<sup>34, 36</sup> One well-documented mechanism underlying MKL1 activation of vascular inflammation is through the p65/NF-κB pathway.<sup>34, 36</sup> Knockdown of *MKL1* in HCASMCs via lentivirus-sh*MKL1* or siRNA pool targeting *MKL1* attenuated the expression of a battery of proinflammatory genes as well as the phosphorylated form of p65 (p-p65) (Figure 5A, 5B). Further, increased p-p65 was seen in HCASMCs transduced with Ad-MKL1 (Figure 5C). These results prompted us to test if *INKILN* promotes the transactivity of MKL1/p65 on the proinflammatory gene program. To test this hypothesis, we first examined the effect of *INKILN* depletion on IL1β-induced p65 nuclear translocation in HASMCs. Western blot of the fractionated protein lysate revealed that IL1β increased the amount of p65 in the chromatin fraction of HASMCs. Such increase was attenuated by siRNA-mediated *INKILN* knockdown. In contrast, neither IL1β stimulation nor *INKILN* knockdown significantly changed p65 protein levels in cytosol or nucleoplasm of HCASMCs (Figure 5D). Similarly, immunostaining showed a reduction of nuclear p65 protein in HCASMCs upon *INKILN* knockdown and IL1β stimulation (Figure



5E). Further, siRNA-mediated *INKILN* knockdown prevented IL1 $\beta$ -induced MKL1 nuclear translocation (Figure 5F). The immunostaining of MKL1 and p65 was authenticated by the species-matched negative control IgG (Figure S5). These results suggest that *INKILN* may be critical for the nuclear interaction between MKL1 and p65 to transactivate the proinflammatory gene program. Consistent with this notion, a significant reduction of TNF $\alpha$ -activated NF- $\kappa$ B reporter activity was seen in HASMCs treated with si*INKILN* (Figure 5G). Collectively, these results support a positive role for *INKILN* in MKL1/p65 transactivation of the proinflammatory gene program.

### Loss of *INKILN* reduces MKL1 protein stability via enhancing ubiquitination proteasome degradation

Data above suggest that MKL1/p65 may mediate *INKILN* activation of the proinflammatory gene program in VSMCs. To further delineate the molecular mechanism, we performed co-immunoprecipitation (Co-IP) in HCASMCs to assess if *INKILN* impacts the interaction between p65 and MKL1, an important mechanism underlying the activation of vascular inflammation.<sup>59</sup> *INKILN* knockdown diminished the association between MKL1 and p65 in HCASMCs. Interestingly, while *INKILN* knockdown displayed no effect on the level of input p65, it caused a notable reduction of the input MKL1, suggesting *INKILN* may positively regulate MKL1 protein abundance (Figure 6A). Indeed, depletion of *INKILN* by two separate siRNAs significantly reduced the protein levels of MKL1 in HCASMCs (Figure 6B). This result was reproduced in HASMCs and RD cells (Figure 6C, 6D). Knockdown of *INKILN* had no effect on *MKL1* mRNA levels (Figure 6E), suggesting that the influence of *INKILN* on MKL1 protein abundance was not attributable to changes in *MKL1* transcription or mRNA stability.

We next considered whether *INKILN* influences MKL1 protein stability. To test this idea, we first assessed whether MKL1 undergoes proteasome-mediated degradation in VSMCs. Incubation of HASMC with a proteasome inhibitor, MG132, significantly increased MKL1 protein levels (Figure 6F), suggesting that MKL1 was subjected to proteasome-mediated protein degradation in VSMCs as reported previously.<sup>37</sup> To ascertain if *INKILN* could impact this process, we depleted *INKILN* in HASMCs with siRNA followed by MG132 treatment. MG132 completely rescued the downregulation of MKL1 protein caused by *INKILN* loss in HCASMCs (Figure 6G). Finally, immunoprecipitation assays revealed that loss of *INKILN* increased the ubiquitinated form of MKL1 compared with that of control siRNA (Figure 6H). These findings suggest that *INKILN* suppresses MKL1 ubiquitination proteasome degradation, leading to elevated levels of MKL1 protein in VSMCs.

### *INKILN* facilitates the interaction between MKL1 and USP10

Ubiquitin proteasome degradation is subjected to the governance of enzyme chains, comprising E1 activating, E2 conjugating, and E3 ligase enzymes, which ultimately leads to the formation of polyubiquitin chains on a target substrate.<sup>60</sup> This process can be reversed by diverse deubiquitinases (DUBs), notably Ubiquitin Specific Peptidase (USP) family members that cleave ubiquitin from ubiquitin-conjugated protein substrates.<sup>61, 62</sup> Among all USP family members, USP10 has emerged as a key regulator of critical biological processes, including immune response and inflammation.<sup>63, 64</sup> To test if USP10 participates in the

de-ubiquitination of MKL1, we first examined if MKL1 physically interacts with USP10 in VSMCs. Co-IP showed MKL1 forms a complex with USP10, a finding further supported by colocalization revealed by immunofluorescence staining (Figure 7A, 7B). Further, siRNA-mediated USP10 knockdown decreased, while adenovirus overexpressing USP10 increased, protein levels of MKL1 in HCASMCs (Figure 7C, 7D). These results suggest that USP10 may serve as a critical DUB to inhibit MKL1 ubiquitination proteasome degradation. To determine how *INKILN* participates in the regulation of USP10 on MKL1 protein, we went on to examine the influence of *INKILN* on USP10 gene expression. Analysis of bulk RNA-seq in *INKILN*-depleted HASMCs failed to reveal a consistent effect of *INKILN* knockdown on the levels of *USP10* mRNA (GSE158219). Western blot showed a marginal, but statistically significant, reduction of USP10 protein levels upon *INKILN* knockdown (Figure 7E). These results suggest that *INKILN* may not have a major role in regulating USP10 expression. We then assessed whether *INKILN* influences the physical interaction between USP10 and MKL1. Co-IP showed that the interaction between MKL1 and USP10 was significantly attenuated by *INKILN* knockdown in HCASMCs (Figure 7F).

Proximity ligation assay (PLA) is a well-recognized approach to determine the physical interactions between proteins.<sup>65</sup> Consistently, PLA revealed a clear interaction between MKL1 and USP10 in HCASMCs, and such interaction was significantly attenuated upon *INKILN* knockdown (Figure 7G). These results suggest that *INKILN* acts as a scaffold to facilitate USP10 deubiquitination of MKL1 protein. The immunostaining of USP10 and PLA for USP10/MKL1 was authenticated by si*USP10* and si*MKL1* (Figure S6A, S6B). Similar to MKL1, there was a clear enrichment of *INKILN* from the RNA precipitates against USP10 antibody but not the negative control IgG in HCASMCs. This interaction appeared to be specific, as lncRNA *NEAT1* was not enriched in the RNA precipitates (Figure 7H). Taken together, these results suggest that *INKILN* stabilizes MKL1 protein through scaffolding MKL1 and USP10, leading to suppression of MKL1 ubiquitin proteasome degradation.

### ***INKILN* expression is induced in diseased vessels of BAC transgenic mice and promotes ligation injury-induced neointimal formation**

Because *INKILN* is a human-specific lncRNA, with no known mouse ortholog, loss-of-function studies in vivo are not possible. To circumvent this limitation, we generated a humanized BAC transgenic mouse strain carrying the *INKILN* and *UMLILO* gene loci, a newly annotated gene (*ENSG00000289530*) found in the first intron of *INKILN*, plus upstream and downstream sequences. Importantly, the neighboring protein-coding gene, *IL8*, was deleted through BAC recombineering; the resultant transgenic mice were genotyped using multiple primers targeting different regions of *INKILN* (Figure S2A, Figure S7A, S7B). Using a newly developed CRISPR-Cas9 long read sequencing (CRISPR-LRS) assay,<sup>49</sup> we mapped this BAC transgene to chromosome 11 at 32,808,215 bp - 32,828,044 bp (mm10) (Figure 8A). qRT-PCR indicated that the BAC integrated as two copies (Figure 8B). CRISPR-LRS libraries found mild genome perturbations on the terminal ends of the tandem transgenes comprised of both human and mouse genome sequences (Figure S7B), a finding consistent with known structural changes at sites of transgene integration.<sup>66</sup> To validate the BAC recombineering, CRISPR-LRS libraries queried inside

of the human BAC. Targeting from the 5' end of *INKILN* through *IL8* revealed successful and exclusive removal of human *IL8* and its proximal promoter. This feature of the *INKILN* BAC mouse allowed us to properly study the function of *INKILN* without the confounding effects of *IL8* expression (Figure S7B). The only protein-coding gene affected in the mouse genome was *Smim23*, a testis-specific gene of unknown function (Figure S7C). We refer to this BAC transgenic (Tg) mouse as BAC *INKILN*Tg. qPCR showed that *INKILN* was undetectable in aortas and carotid arteries under physiological conditions, but robustly induced in ex vivo cultured aortas and carotid arteries subjected to complete ligation (Figure 8C, 8D). There was no detectable *UMLILO* or ENSG00000289530 gene expression under these conditions (**data not shown**). The injury-induced *INKILN* expression in the carotids was further validated by RNA FISH using a specific probe to *INKILN* (Figure 8E). Further, *INKILN* was robustly induced by lipopolysaccharide (LPS) in bone marrow-derived macrophages (BMDMs) from *INKILN*Tg mice (Figure S7D). Finally, immuno-RNA FISH confirmed the colocalization of *INKILN* and mouse MKL1 protein in these LPS-induced BMDMs, suggesting a similar physical interaction between *INKILN* and MKL1 in BAC *INKILN*Tg mice (Figure S7E). These results are congruent with the induction of *INKILN* in phenotypically modulated human SMCs and in atherosclerotic and aneurysmal human vessels.

Finally, we sought to determine the influence of *INKILN* on ligation injury-induced neointimal formation in *INKILN*Tg mice. We subjected *INKILN*Tg and littermate WT control mice to left carotid artery ligation injury for 3 weeks. H&E staining of the serial sections at defined distances from the ligation suture site showed significantly increased neointimal formation in the distal region (level 3) of *INKILN*Tg mice relative to littermate WT control mice; comparable neointimal formation was seen in level 1 and level 2 regions of *INKILN*Tg and littermate WT control mice (Figure 8F, 8G). No discernable difference was observed in the medial layer of injured and sham control carotids in *INKILN*Tg versus WT mice (Figure S7F). Immunostaining showed increased proinflammatory cell infiltration and cell proliferation, with increased cell numbers positive for macrophage marker MAC2, leukocyte marker CD45, and proliferation marker KI67, respectively, in the injured carotids of *INKILN*Tg mice relative to WT controls (Figure 8H). We did not observe significant changes in ACTA2 positive cells in the injured vessels from Tg versus WT mice (Figure 8H). Authentication of MAC2 and CD45 staining was conducted using species-matched IgG controls (Figure S7G). Finally, ligation injured carotids exhibited significantly higher levels of MKL1 protein compared with those in WT mice, suggesting a similar effect of *INKILN* on MKL1 protein stability in *INKILN*Tg mice (Figure 8I). These results demonstrate that *INKILN* is induced in the context of vascular injury and exacerbates neointimal formation, consistent with results seen in human cells and vessels.

## Discussion

The present study provides insight into the transcriptional control, proinflammatory role, and mechanistic action of a novel, human-specific lncRNA, *INKILN*, in VSMCs. Evidence is provided for *INKILN* downregulation in differentiated contractile VSMCs and upregulation upon proinflammatory stimuli in a p65/NFκB-dependent manner. *INKILN* activates the proinflammatory gene program in multiple primary VSMCs and ex vivo HSV

cultures, and promotes injury-induced neointimal formation in BAC *INKILN*Tg mice. The molecular basis underlying *INKILN* activation of VSMC inflammation involves its action as a scaffold with MKL1, a major transcriptional activator of vascular inflammation, and the deubiquitinase USP10, which inhibits MKL1 ubiquitination and proteasomal degradation (Figure 8J). Our study not only uncovers a novel lncRNA activating the VSMC proinflammatory phenotype, but also elucidates a previously unknown pathway governing MKL1 protein stability to potentiate its proinflammatory role. Given the increased recognition of VSMC phenotypic switching to macrophage-like proinflammatory phenotype in the initiation and aggravation of vascular diseases,<sup>67</sup> our study provides important insights into potential therapeutic strategies for vascular diseases via effectively targeting the interplay between coding and noncoding pathways. Because the induction and function of *INKILN* in BAC Tg mice recapitulate those in human cells and tissues, our study also indicates that human BAC Tg mouse models may offer an innovative approach to studying human-specific lncRNAs in the vascular system.

The genomic localization of *INKILN* is particularly unique, with its first intron harboring the upstream master lncRNA of the inflammatory chemokine locus (*UMLILO*) transcribed in a reverse direction. *UMLILO* is an enhancer lncRNA that facilitates H3K4me3 epigenetic priming of chemokine genes and trained immunity.<sup>68</sup> *UMLILO* is barely detectable in our VSMC systems (data not shown). This suggests that the functional role of *INKILN* may be independent of *UMLILO*. It should be noted, though *INKILN* and *UMLILO* reside in the same enhancer RNA region on chromosome 4 and both activate proinflammatory genes, several distinctions exist. First, no overlapping sequence is seen in their annotated transcripts. Second, *INKILN* loss-of-function has no effect on *UMLILO* expression (Figure S8). Third, *INKILN* is predominately located in the cytosolic compartment whereas *UMLILO* resides in the nucleus. Finally, *UMLILO* activates chemokine genes in *cis*, whose activity is confined to a *CXCL* topologically associated domain.<sup>68</sup> In contrast, *INKILN* functions in the cytosol and influences a broad range of proinflammatory genes. Therefore, though regulatory roles exerted by these two human-specific lncRNAs appear similar in triggering inflammation, they utilize distinct pathways to achieve functional consequences. Among all lncRNAs annotated in the human genome, the majority of them are restricted to humans. This is particularly true for lncRNAs identified as modulators of immune and inflammatory responses, including previously published *NKILA*, *lncRNA-CCL2*, *INCR1*, and *LUCATI*.<sup>23, 69–71</sup> These human-specific immune and inflammatory regulatory lncRNAs could underlie the complexity of immune responses and inflammatory diseases occurring in humans, but not in rodents.

The nearest neighboring protein coding gene to the *INKILN* locus is *IL8*, which is located 20 kb upstream of *INKILN* with no annotated intervening genes. We thus consider *INKILN* and *IL8* as a coding and noncoding gene pair. As a human specific prototypic chemokine, IL8 plays a vital role in inflammation initiation and immune cell chemotaxis, contributing to the pathogenesis of various inflammatory diseases, such as infectious disease, chronic obstructive pulmonary disease, asthma, and cancer.<sup>72–75</sup> Therefore, inhibition of *IL8* gene expression has emerged as an appealing strategy for therapies against these diseases.<sup>73, 76, 77</sup> Previous studies reported that *IL8* gene activation involves three distinct regulatory mechanisms: (1) de-repression of the promoter operated by multiple repressors, such as

NF- $\kappa$ B-repressing factor, octamer-1 (OCT-1), and HDAC1; (2) transactivation by NF- $\kappa$ B and AP1; and (3) mRNA stabilization by the p38MAPK pathway.<sup>78</sup> In our current study, we showed that *INKILN* positively regulates *IL8* gene expression, which is consistent with our recent survey wherein a connection between *IL8* and *INKILN* was suggested.<sup>79</sup> This finding together with the epigenetic activation of *IL8* by the enhancer lncRNA *UMLILO*, implies a new lncRNA-mediated regulatory mechanism underlying *IL8* gene activation, which will have important implications for effectively targeting *IL8* gene expression for therapy. Elegant studies from Dr. Wang's lab, using an innovative transgenic mouse model, which carries a 166 kilobase BAC encompassing the entire human *IL8* gene locus, have reported a crucial role for IL8 in aggravating inflammation and gastrointestinal tumor formation.<sup>80</sup> Of note, beyond *IL8*, this BAC also harbors the gene loci of *INKILN*, *UMLILO*, and *ENSG00000289530*. Given the genomic complexity of the BAC insert, the influence of each of these gene products on phenotypes seen in BAC transgenic mice should be taken into account. Finally, careful analysis of the chromatin landscape of *INKILN* and *IL8* revealed multiple peaks of active epigenetic markers, such as H3K27ac and H3K4Me1, suggesting potential enhancers that participate in the transactivation of both genes (Figure S2A). The transcription of both *INKILN* and *IL8* is likely subjected to their individual NF- $\kappa$ B site(s) identified in their proximal promoter regions reported here and in previous studies.<sup>78</sup> Elucidating the in vivo functional role of these regulatory sites awaits future investigative work using genome editing tools as shown for other control elements effecting lncRNA gene expression.<sup>46, 47</sup>

It has long been recognized that the action of MKL1 on transcriptional regulation is signal-responsive and tightly modulated by actin dynamics involving its nucleocytoplasmic translocation.<sup>58, 81</sup> In addition, recent studies have reported that MKL1 can also modulate gene expression through epigenetic pathways, mainly by interacting with multiple histone modifiers, including Brahma-related gene-1 (BRG1), COMPASS/COMPASS-like complex, and WD Repeat Domain 5 (WDR5), to ensure an active chromatin status for gene transcription.<sup>35, 82, 83</sup> Compared with these well-established mechanisms underlying MKL1 transactivity, the regulation of MKL1 expression, especially at the protein level, is limited.<sup>37</sup> Here, we report on a novel paradigm for MKL1 protein stability, which involves the coordinated actions of *INKILN* and the deubiquitinase USP10 in the cytoplasm. The fact that *INKILN* depletion results in a decreased interaction between MKL1 and USP10 suggests that *INKILN* acts as a scaffold for USP10 and MKL1 to facilitate USP10-mediated deubiquitination of MKL1. Given the increased levels of *INKILN* expression reported here and MKL1 protein under vascular disease contexts such as aortic dissection and aneurysm,<sup>33, 34</sup> we propose *INKILN* serves as a previously unknown mechanism underlying MKL1 protein stability during disease progression. The detailed mechanism as to how the regulatory axis of *INKILN*/USP10/MKL1 operates to stabilize MKL1 protein awaits further investigation.

One distinct paradigm derived from our current study is utilization of human BAC Tg mice for elucidating the vascular disease-associated regulation and function of human-specific non-conserved lncRNAs. The majority of transcribed lncRNAs in the human genome are human-specific, lacking orthologs in rodents. Bioinformatics studies suggest that up to 2/3 of non-conserved human-specific long intergenic ncRNAs (lincRNAs) are associated



with cardiometabolic traits.<sup>12</sup> In vivo characterization of those human-specific lncRNAs in a physiological manner represents a big challenge. In our current study, we generated a human BAC which carries the intact *INKILN* gene locus and surrounding sequences, providing a physiologically relevant genomic milieu for *INKILN* gene transcription. The gene expression pattern of *INKILN* in Tg mice mirrors *INKILN* in human cells and tissues, indicating the human BAC Tg mouse captures critical regulatory elements required for *INKILN* transcription. Notably, we observed a significant increase in neointimal formation in *INKILN* Tg mice, which is in line with the proinflammatory function of *INKILN* in humans. These results suggest that humanized BAC Tg mice may offer a physiologically relevant tool for in vivo investigation of human specific lncRNAs, whose studies currently are largely confined to in vitro cultured cells.<sup>13</sup> To our knowledge, this is the first report harnessing human BAC Tg mice to investigate the function of a non-conserved human lncRNA in the vascular system.

Several lines of key evidence are provided to support the proinflammatory role of *INKILN* in VSMCs. First, *INKILN* is highly induced in cultured VSMCs by different proinflammatory stimuli, ex vivo cultured HSV segments, and human aneurysm samples. Second, both loss-of-function and gain-of-function studies consistently revealed a positive role for *INKILN* in activating a repertoire of proinflammatory genes. Third, loss of *INKILN* reduced the interaction between p65 and MKL1 protein and the transactivity of p65/NF- $\kappa$ B. These data collectively suggest a novel regulatory axis comprising *INKILN*, MKL1, and p65 to potentiate the proinflammatory gene program in VSMCs. The attenuation of MKL1 nuclear translocation upon *INKILN* depletion is intriguing, and may be partially attributable to the decreased MKL1 protein pool. In addition, beyond the cytosolic interaction with USP10 and MKL1 to stabilize MKL1 protein, *INKILN* could sequester away G-actin for MKL1 binding, thereby releasing MKL1 for nuclear shuttling. On the other hand, though the reduced p65 nuclear translocation was consistently seen in VSMCs with *INKILN* knockdown, we could not detect the physical association between *INKILN* and p65 in our system. We thus surmise that the impact of *INKILN* on p65 nuclear translocation is likely indirect. One possibility is the influence of the proinflammatory cytokines and chemokines that are activated by *INKILN*.

There are several limitations in our current study. First, the NF- $\kappa$ B site we defined only exhibited moderate response to TNF $\alpha$  treatment. Given the robust activation of *INKILN* gene expression in response to TNF $\alpha$ , additional *cis* element(s) may be responsible for *INKILN* gene transcription. Second, additional mechanisms may underlie *INKILN*-induced activation of proinflammatory gene expression. Third, despite repeated attempts, the physical interaction between *INKILN* and MKL1/USP10 in patient samples and animal models is lacking. Newer assays and reagents will be necessary to overcome the technical challenges in demonstrating such in vivo complexes. Though expression of *UMLILO* and a newly annotated gene *ENSG00000289530* are undetectable in vascular cells and Tg mice under conditions of *INKILN* expression (data not shown), the influence on the phenotype of Tg mice through an indirect pathway, for example via *cis* regulatory pathway, cannot be excluded. Finally, precise elucidation of *INKILN* gene transcription using genome editing approaches cannot be easily conducted with current *INKILN* Tg mice because of two tandem copies of *INKILN*.

In summary, we report the novel lncRNA *INKILN* as a potent activator of VSMC inflammation. The proinflammatory action of *INKILN* is, at least partially, mediated by scaffolding MKL1 and USP10, thereby alleviating MKL1 ubiquitination-mediated proteasome degradation. *INKILN* is the first lncRNA identified that interacts with and stabilizes MKL1 protein to activate VSMC inflammation. Given the emerging roles of VSMC inflammation, and well-recognized role of the VSMC phenotypic switching to macrophage-like transition in the etiology of different vascular disorders,<sup>67</sup> our findings provide new insights into a therapeutic strategy for vascular disease via effectively targeting the interplay between coding and noncoding pathways. Our studies also indicate that human BAC Tg mouse models offer a novel approach for in vivo investigation of human specific lncRNAs in a physiological relevant genomic context.

## Supplementary Material

Refer to Web version on PubMed Central for supplementary material.

## Acknowledgements

We thank Rochester Genomics Research Center for performing the RNA-seq experiments and Dr. Deyou Zheng from Albert Einstein College of Medicine for bioinformatics analysis. We thank cell culture core at Albany Medical College for providing us with the primary HSV SMC cultures.

## Sources of Funding

This work is supported in part by R01 grants from National Institutes of Health (HL122686 and HL139794 to Dr. Long; HL138987 and HL147476 to Dr. Miano; HL148239 and HL164577 to Dr. Miller; AG076235 and HL142097 to Dr. Weintraub; and CA250636 to Dr. Barroso) and grants from American Heart Association (EIA961515 to Dr. Long; CDA34110319 to Dr. Zhang; 863622 and 971459 to Dr. Weintraub; Predoctoral Fellowship PRE34380659 to Dr. Gao; and Postdoctoral Fellowship 915887 to Dr. Ishimwe). Dr. Baker is supported by European Research Council 338991 VASMIR (European Research Council Advanced Grant 338991) and British Heart Foundation (BHF) Chair and Programme grants (CH/11/2/28733, RG/14/3/30706, and RG/20/5/34796). Dr. Maegdefessel is supported by the German Center for Cardiovascular Research (DZHK; Junior Research Group), the SFB1123 and TRR267 of the German Research Council (DFG), and the Swedish Research Council (Vetenkapsradet, 2019-01577).

## Nonstandard Abbreviations and Acronyms

<b>BAC</b>	Bacterial Artificial Chromosome
<b>ChIP</b>	Chromatin immunoprecipitation
<b>CRISPR-LRS</b>	CRISPR-Cas9 long-read sequencing
<b>DUB</b>	Deubiquitinase
<b>FISH</b>	Fluorescence in situ hybridization
<b>HASMC</b>	Human aortic smooth muscle cell
<b>HCAMSC</b>	Human coronary artery smooth muscle cell
<b>HSV</b>	Human saphenous vein
<b><i>INKILN</i></b>	INflammatory MKL1 Interacting Long Noncoding RNA

<b>Jpk</b>	Jasplakinolide
<b>LncRNA</b>	Long noncoding RNA
<b>MKL1</b>	Megakaryoblastic leukemia 1
<b>PLA</b>	Proximity ligation assay
<b>RIP</b>	RNA immunoprecipitation
<b>Tg</b>	Transgenic
<b>USP10</b>	Ubiquitin Specific Peptidase 10
<b>VSMC</b>	Vascular smooth muscle cell

## References

- Zanoli L, Briet M, Empana JP, Cunha PG, Mäki-Petäjä KM, Protogerou AD, Tedgui A, Touyz RM, Schiffrin EL, Spronck B, Bouchard P, Vlachopoulos C, Bruno RM and Boutouyrie P. Vascular consequences of inflammation: a position statement from the ESH Working Group on Vascular Structure and Function and the ARTERY Society. *J Hypertens*. 2020;38:1682–1698. [PubMed: 32649623]
- Shah PK. Inflammation, neointimal hyperplasia, and restenosis: as the leukocytes roll, the arteries thicken. *Circulation*. 2003;107:2175–7. [PubMed: 12732592]
- Williams JW, Huang LH and Randolph GJ. Cytokine Circuits in Cardiovascular Disease. *Immunity*. 2019;50:941–954. [PubMed: 30995508]
- Liberale L, Ministrini S, Carbone F, Camici GG and Montecucco F. Cytokines as therapeutic targets for cardio- and cerebrovascular diseases. *Basic Res Cardiol*. 2021;116:23. [PubMed: 33770265]
- Nguyen MT, Fernando S, Schwarz N, Tan JT, Bursill CA and Psaltis PJ. Inflammation as a Therapeutic Target in Atherosclerosis. *J Clin Med*. 2019;8.
- Libby P and Everett BM. Novel Antiatherosclerotic Therapies. *Arteriosclerosis, thrombosis, and vascular biology*. 2019;39:538–545. [PubMed: 30816799]
- Baylis RA, Gomez D, Mallat Z, Pasterkamp G and Owens GK. The CANTOS Trial: One Important Step for Clinical Cardiology but a Giant Leap for Vascular Biology. *Arteriosclerosis, thrombosis, and vascular biology*. 2017;37:e174–e177. [PubMed: 28970294]
- Kosmas CE, Silverio D, Sourlas A, Montan PD, Guzman E and Garcia MJ. Anti-inflammatory therapy for cardiovascular disease. *Ann Transl Med*. 2019;7:147. [PubMed: 31157268]
- Ridker PM. Anti-inflammatory therapy for atherosclerosis: interpreting divergent results from the CANTOS and CIRT clinical trials. *J Intern Med*. 2019;285:503–509. [PubMed: 30472762]
- Wapinski O and Chang HY. Long noncoding RNAs and human disease. *Trends Cell Biol*. 2011;6:354–361.
- Fatica A and Bozzoni I. Long non-coding RNAs: new players in cell differentiation and development. *Nat Rev Genet*. 2014;15:7–21. [PubMed: 24296535]
- Foulkes AS, Selvaggi C, Cao T, O'Reilly ME, Cynn E, Ma P, Lumish H, Xue C and Reilly MP. Nonconserved Long Intergenic Noncoding RNAs Associate With Complex Cardiometabolic Disease Traits. *Arteriosclerosis, thrombosis, and vascular biology*. 2021;41:501–511. [PubMed: 33176448]
- Ghanam AR, Bryant WB, Miano JM. Of mice and human-specific long noncoding RNAs. *Mamm Genome*. 2022;33:281–292. [PubMed: 35106622]
- Andersen RE, Hong SJ, Lim JJ, Cui M, Harpur BA, Hwang E, Delgado RN, Ramos AD, Liu SJ, Blencowe BJ and Lim DA. The Long Noncoding RNA Pnky Is a Trans-acting Regulator of Cortical Development In Vivo. *Developmental cell*. 2019;49:632–642.e7. [PubMed: 31112699]

15. Statello L, Guo CJ, Chen LL and Huarte M. Gene regulation by long non-coding RNAs and its biological functions. *Nature reviews Molecular cell biology*. 2021;22:96–118. [PubMed: 33353982]
16. Jaé N and Dimmeler S. Noncoding RNAs in Vascular Diseases. *Circulation research*. 2020;126:1127–1145. [PubMed: 32324505]
17. Zhao J, Zhang W, Lin M, Wu W, Jiang P, Tou E, Xue M, Richards A, Jourd'heuil D, Asif A, Zheng D, Singer HA, Miano JM and Long X. MYOSLID Is a Novel Serum Response Factor-Dependent Long Noncoding RNA That Amplifies the Vascular Smooth Muscle Differentiation Program. *Arteriosclerosis, thrombosis, and vascular biology*. 2016;36:2088–99. [PubMed: 27444199]
18. Leisegang MS, Fork C, Jospovic I, Richter FM, Preussner J, Hu J, Miller MJ, Epah J, Hofmann P, Günther S, Moll F, Valasarajan C, Heidler J, Ponomareva Y, Freiman TM, Maegdefessel L, Plate KH, Mittelbronn M, Uchida S, Künnle C, Stellos K, Schermuly RT, Weissmann N, Devraj K, Wittig I, Boon RA, Dimmeler S, Pullamsetti SS, Looso M, Miller FJ, Jr. and Brandes RP. Long Noncoding RNA MANTIS Facilitates Endothelial Angiogenic Function. *Circulation*. 2017;136:65–79. [PubMed: 28351900]
19. Das S, Zhang E, Senapati P, Amaram V, Reddy MA, Stapleton K, Leung A, Lanting L, Wang M, Chen Z, Kato M, Oh HJ, Guo Q, Zhang X, Zhang B, Zhang H, Zhao Q, Wang W, Wu Y and Natarajan R. A Novel Angiotensin II-Induced Long Noncoding RNA Giver Regulates Oxidative Stress, Inflammation, and Proliferation in Vascular Smooth Muscle Cells. *Circulation research*. 2018;123:1298–1312. [PubMed: 30566058]
20. Haemmig S, Yang D, Sun X, Das D, Ghaffari S, Molinaro R, Chen L, Deng Y, Freeman D, Moullan N, Tesmenitsky Y, Wara A, Simion V, Shvartz E, Lee JF, Yang T, Sukova G, Marto JA, Stone PH, Lee WL, Auwerx J, Libby P and Feinberg MW. Long noncoding RNA SNHG12 integrates a DNA-PK-mediated DNA damage response and vascular senescence. *Science translational medicine*. 2020;12.
21. Monteiro JP, Rodor J, Caudrillier A, Scanlon JP, Spiroski AM, Dudnakova T, Pflüger-Müller B, Shmakova A, von Kriegsheim A, Deng L, Taylor RS, Wilson-Kanamori JR, Chen SH, Stewart K, Thomson A, Miti T, McClure JD, Iynikell J, Hadoke PWF, Denby L, Bradshaw AC, Caruso P, Morrell NW, Kovacic JC, Ulitsky I, Henderson NC, Caporali A, Leisegang MS, Brandes RP and Baker AH. MIR503HG Loss Promotes Endothelial-to-Mesenchymal Transition in Vascular Disease. *Circulation research*. 2021;128:1173–1190. [PubMed: 33703914]
22. Lyu Q, Xu S, Lyu Y, Choi M, Christie CK, Slivano OJ, Rahman A, Jin ZG, Long X, Xu Y and Miano JM. SENCER stabilizes vascular endothelial cell adherens junctions through interaction with CKAP4. *Proceedings of the National Academy of Sciences of the United States of America*. 2019;116:546–555. [PubMed: 30584103]
23. Khyzha N, Khor M, DiStefano PV, Wang L, Matic L, Hedin U, Wilson MD, Maegdefessel L and Fish JE. Regulation of CCL2 expression in human vascular endothelial cells by a neighboring divergently transcribed long noncoding RNA. *Proceedings of the National Academy of Sciences of the United States of America*. 2019;116:16410–16419. [PubMed: 31350345]
24. Simion V, Zhou H, Pierce JB, Yang D, Haemmig S, Tesmenitsky Y, Sukhova G, Stone PH, Libby P and Feinberg MW. LncRNA VINAS regulates atherosclerosis by modulating NF- $\kappa$ B and MAPK signaling. *JCI insight*. 2020;5.
25. Cremer S, Michalik KM, Fischer A, Pfisterer L, Jaé N, Winter C, Boon RA, Muhly-Reinholz M, John D, Uchida S, Weber C, Poller W, Günther S, Braun T, Li DY, Maegdefessel L, Perisic Matic L, Hedin U, Soehnlein O, Zeiher A and Dimmeler S. Hematopoietic Deficiency of the Long Noncoding RNA MALAT1 Promotes Atherosclerosis and Plaque Inflammation. *Circulation*. 2019;139:1320–1334. [PubMed: 30586743]
26. Chen Y, Zhao X and Wu H. Transcriptional Programming in Arteriosclerotic Disease: A Multifaceted Function of the Runx2 (Runt-Related Transcription Factor 2). *Arteriosclerosis, thrombosis, and vascular biology*. 2021;41:20–34. [PubMed: 33115268]
27. Wang DZ, Li S, Hockemeyer D, Sutherland L, Wang Z, Schrott G, Richardson JA, Nordheim A and Olson EN. Potentiation of serum response factor activity by a family of myocardin-related transcription factors. *Proceedings of the National Academy of Sciences of the United States of America*. 2002;99:14855–60. [PubMed: 12397177]

28. Du KL, Chen M, Li J, Lepore JJ, Mericko P and Parmacek MS. Megakaryoblastic leukemia factor-1 transduces cytoskeletal signals and induces smooth muscle cell differentiation from undifferentiated embryonic stem cells. *J Biol Chem.* 2004;279:17578–86. [PubMed: 14970199]
29. Parmacek MS. Myocardin-related transcription factors: critical coactivators regulating cardiovascular development and adaptation. *Circulation research.* 2007;100:633–44. [PubMed: 17363709]
30. Minami T, Kuwahara K, Nakagawa Y, Takaoka M, Kinoshita H, Nakao K, Kuwabara Y, Yamada Y, Yamada C, Shibata J, Usami S, Yasuno S, Nishikimi T, Ueshima K, Sata M, Nakano H, Seno T, Kawahito Y, Sobue K, Kimura A, Nagai R and Nakao K. Reciprocal expression of MRTF-A and myocardin is crucial for pathological vascular remodelling in mice. *Embo j.* 2012;31:4428–40. [PubMed: 23103763]
31. An J, Naruse TK, Hinohara K, Soejima Y, Sawabe M, Nakagawa Y, Kuwahara K and Kimura A. MRTF-A regulates proliferation and survival properties of pro-atherogenic macrophages. *Journal of molecular and cellular cardiology.* 2019;133:26–35. [PubMed: 31128166]
32. Chen D, Yang Y, Cheng X, Fang F, Xu G, Yuan Z, Xia J, Kong H, Xie W, Wang H, Fang M, Gao Y and Xu Y. Megakaryocytic leukemia 1 directs a histone H3 lysine 4 methyltransferase complex to regulate hypoxic pulmonary hypertension. *Hypertension.* 2015;65:821–33. [PubMed: 25646298]
33. Ito S, Hashimoto Y, Majima R, Nakao E, Aoki H, Nishihara M, Ohno-Urabe S, Furusho A, Hirakata S, Nishida N, Hayashi M, Kuwahara K and Fukumoto Y. MRTF-A promotes angiotensin II-induced inflammatory response and aortic dissection in mice. *PLoS one.* 2020;15:e0229888. [PubMed: 32208430]
34. Gao P, Gao P, Zhao J, Shan S, Luo W, Slivano OJ, Zhang W, Tabuchi A, LeMaire SA, Maegdefessel L, Shen YH, Miano JM, Singer HA and Long X. MKL1 cooperates with p38MAPK to promote vascular senescence, inflammation, and abdominal aortic aneurysm. *Redox biology.* 2021;41:101903. [PubMed: 33667992]
35. Yang Y, Chen D, Yuan Z, Fang F, Cheng X, Xia J, Fang M, Xu Y and Gao Y. Megakaryocytic leukemia 1 (MKL1) ties the epigenetic machinery to hypoxia-induced transactivation of endothelin-1. *Nucleic Acids Res.* 2013;41:6005–17. [PubMed: 23625963]
36. Yu L, Fang F, Dai X, Xu H, Qi X, Fang M and Xu Y. MKL1 defines the H3K4Me3 landscape for NF- $\kappa$ B dependent inflammatory response. *Sci Rep.* 2017;7:191. [PubMed: 28298643]
37. Hinson JS, Medlin MD, Taylor JM and Mack CP. Regulation of myocardin factor protein stability by the LIM-only protein FHL2. *American journal of physiology Heart and circulatory physiology.* 2008;295:H1067–h1075. [PubMed: 18586895]
38. Wu W, Zhang W, Choi M, Zhao J, Gao P, Xue M, Singer HA, Jourdeuil D and Long X. Vascular smooth muscle-MAPK14 is required for neointimal hyperplasia by suppressing VSMC differentiation and inducing proliferation and inflammation. *Redox biology.* 2019;22:101137. [PubMed: 30771750]
39. Mahmoud AD, Ballantyne MD, Miscianinov V, Pinel K, Hung J, Scanlon JP, Iyinnikel J, Kaczynski J, Tavares AS, Bradshaw AC, Mills NL, Newby DE, Caporali A, Gould GW, George SJ, Ulitsky I, Sluimer JC, Rodor J and Baker AH. The Human-Specific and Smooth Muscle Cell-Enriched LncRNA SMILR Promotes Proliferation by Regulating Mitotic CENPF mRNA and Drives Cell-Cycle Progression Which Can Be Targeted to Limit Vascular Remodeling. *Circulation research.* 2019;125:535–551. [PubMed: 31339449]
40. Turner AW, Hu SS, Mosquera JV, Ma WF, Hodonsky CJ, Wong D, Auguste G, Song Y, Sol-Church K, Farber E, Kundu S, Kundaje A, Lopez NG, Ma L, Ghosh SKB, Onengut-Gumuscu S, Ashley EA, Quertermous T, Finn AV, Leeper NJ, Kovacic JC, Björkegren JLM, Zang C and Miller CL. Single-nucleus chromatin accessibility profiling highlights regulatory mechanisms of coronary artery disease risk. *Nat Genet.* 2022;54:804–816. [PubMed: 35590109]
41. Corces MR, Trevino AE, Hamilton EG, Greenside PG, Sinnott-Armstrong NA, Vesuna S, Satpathy AT, Rubin AJ, Montine KS, Wu B, Kathiria A, Cho SW, Mumbach MR, Carter AC, Kasowski M, Orloff LA, Risca VI, Kundaje A, Khavari PA, Montine TJ, Greenleaf WJ and Chang HY. An improved ATAC-seq protocol reduces background and enables interrogation of frozen tissues. *Nature methods.* 2017;14:959–962. [PubMed: 28846090]



42. Granja JM, Corces MR, Pierce SE, Bagdatli ST, Choudhry H, Chang HY and Greenleaf WJ. ArchR is a scalable software package for integrative single-cell chromatin accessibility analysis. *Nat Genet.* 2021;53:403–411. [PubMed: 33633365]
43. Wirka RC, Wagh D, Paik DT, Pjanic M, Nguyen T, Miller CL, Kundu R, Nagao M, Collier J, Koyano TK, Fong R, Woo YJ, Liu B, Montgomery SB, Wu JC, Zhu K, Chang R, Alamprese M, Tallquist MD, Kim JB and Quertermous T. Atheroprotective roles of smooth muscle cell phenotypic modulation and the TCF21 disease gene as revealed by single-cell analysis. *Nature medicine.* 2019;25:1280–1289.
44. Long X and Miano JM. Transforming growth factor-beta1 (TGF-beta1) utilizes distinct pathways for the transcriptional activation of microRNA 143/145 in human coronary artery smooth muscle cells. *J Biol Chem.* 2011;286:30119–29. [PubMed: 21712382]
45. Fasolo F, Jin H, Winski G, Chernogubova E, Pauli J, Winter H, Li DY, Glukha N, Bauer S, Metschl S, Wu Z, Koschinsky ML, Reilly M, Pelisek J, Kempf W, Eckstein HH, Soehnlein O, Matic L, Hedin U, Bäcklund A, Bergmark C, Paloschi V and Maegdefessel L. Long Noncoding RNA MIAT Controls Advanced Atherosclerotic Lesion Formation and Plaque Destabilization. *Circulation.* 2021;144:1567–1583. [PubMed: 34647815]
46. Gao P, Lyu Q, Ghanam AR, Lazzarotto CR, Newby GA, Zhang W, Choi M, Slivano OJ, Holden K, Walker JA 2nd, Kadina AP, Munroe RJ, Abratte CM, Schimenti JC, Liu DR, Tsai SQ, Long X and Miano JM. Prime editing in mice reveals the essentiality of a single base in driving tissue-specific gene expression. *Genome biology.* 2021;22:83. [PubMed: 33722289]
47. Choi M, Lu YW, Zhao J, Wu M, Zhang W and Long X. Transcriptional control of a novel long noncoding RNA Mym1 in smooth muscle cells by a single Cis-element and its initial functional characterization in vessels. *Journal of molecular and cellular cardiology.* 2020;138:147–157. [PubMed: 31751568]
48. Zhao J, Wu W, Zhang W, Lu YW, Tou E, Ye J, Gao P, Jourdeuil D, Singer HA, Wu M and Long X. Selective expression of TSPAN2 in vascular smooth muscle is independently regulated by TGF-beta1/SMAD and myocardin/serum response factor. *FASEB J.* 2017;31:2576–2591. [PubMed: 28258189]
49. Bryant WB, Yang A, Griffin S, Zhang W, Long X and Miano JM. CRISPR-Cas9 long read sequencing for mapping transgenes in the mouse genome. *The CRISPR J.* 2023;6:163–175. [PubMed: 37071672]
50. Chen J, Kitchen CM, Streb JW and Miano JM. Myocardin: a component of a molecular switch for smooth muscle differentiation. *Journal of molecular and cellular cardiology.* 2002;34:1345–56. [PubMed: 12392995]
51. Hon CC, Ramilowski JA, Harshbarger J, Bertin N, Rackham OJ, Gough J, Denisenko E, Schmeier S, Poulsen TM, Severin J, Lizio M, Kawaji H, Kasukawa T, Itoh M, Burroughs AM, Noma S, Djebali S, Alam T, Medvedeva YA, Testa AC, Lipovich L, Yip CW, Abugessaisa I, Mendez M, Hasegawa A, Tang D, Lassmann T, Heutink P, Babina M, Wells CA, Kojima S, Nakamura Y, Suzuki H, Daub CO, de Hoon MJ, Arner E, Hayashizaki Y, Carninci P and Forrest AR. An atlas of human long non-coding RNAs with accurate 5' ends. *Nature.* 2017;543:199–204. [PubMed: 28241135]
52. Tang Y, Yang X, Friesel RE, Vary CP and Liaw L. Mechanisms of TGF-beta-induced differentiation in human vascular smooth muscle cells. *Journal of vascular research.* 2011;48:485–94. [PubMed: 21832838]
53. Sobue K, Hayashi K, Nishida W. Expression regulation of smooth muscle cell-specific genes in association with phenotypic modulation. *Mol Cell Biochem.* 1999;190:105–118. [PubMed: 10098977]
54. Ballantyne MD, Pinel K, Dakin R, Vesey AT, Diver L, Mackenzie R, Garcia R, Welsh P, Sattar N, Hamilton G, Joshi N, Dweck MR, Miano JM, McBride MW, Newby DE, McDonald RA and Baker AH. Smooth Muscle Enriched Long Noncoding RNA (SMILR) Regulates Cell Proliferation. *Circulation.* 2016;133:2050–65. [PubMed: 27052414]
55. Harshe RP, Xie A, Vuerich M, Frank LA, Gromova B, Zhang H, Robles RJ, Mukherjee S, Csizmadia E, Kokkotou E, Cheifetz AS, Moss AC, Kota SK, Robson SC and Longhi MS. Endogenous antisense RNA curbs CD39 expression in Crohn's disease. *Nat Commun.* 2020;11:5894. [PubMed: 33208731]

56. Kalota A, Karabon L, Swider CR, Viazovkina E, Elzagheid M, Damha MJ and Gewirtz AM. 2'-deoxy-2'-fluoro-beta-D-arabinonucleic acid (2'F-ANA) modified oligonucleotides (ON) effect highly efficient, and persistent, gene silencing. *Nucleic Acids Res.* 2006;34:451–61. [PubMed: 16421272]
57. Agostini F, Zanzoni A, Klus P, Marchese D, Cirillo D and Tartaglia GG. catRAPID omics: a web server for large-scale prediction of protein-RNA interactions. *Bioinformatics (Oxford, England).* 2013;29:2928–30. [PubMed: 23975767]
58. Olson EN and Nordheim A. Linking actin dynamics and gene transcription to drive cellular motile functions. *Nature reviews Molecular cell biology.* 2010;11:353–65. [PubMed: 20414257]
59. Fang F, Yang Y, Yuan Z, Gao Y, Zhou J, Chen Q and Xu Y. Myocardin-related transcription factor A mediates OxLDL-induced endothelial injury. *Circulation research.* 2011;108:797–807. [PubMed: 21330600]
60. Senft D, Qi J and Ronai ZA. Ubiquitin ligases in oncogenic transformation and cancer therapy. *Nature reviews Cancer.* 2018;18:69–88. [PubMed: 29242641]
61. Bhattacharya U, Neizer-Ashun F, Mukherjee P and Bhattacharya R. When the chains do not break: the role of USP10 in physiology and pathology. *Cell death & disease.* 2020;11:1033. [PubMed: 33277473]
62. Leung I, Dekel A, Shifman JM and Sidhu SS. Saturation scanning of ubiquitin variants reveals a common hot spot for binding to USP2 and USP21. *Proceedings of the National Academy of Sciences of the United States of America.* 2016;113:8705–10. [PubMed: 27436899]
63. Wang L, Wu D and Xu Z. USP10 protects against cerebral ischemia injury by suppressing inflammation and apoptosis through the inhibition of TAK1 signaling. *Biochem Biophys Res Commun.* 2019;516:1272–1278. [PubMed: 31301769]
64. Luo P, Qin C, Zhu L, Fang C, Zhang Y, Zhang H, Pei F, Tian S, Zhu XY, Gong J, Mao Q, Xiao C, Su Y, Zheng H, Xu T, Lu J and Zhang J. Ubiquitin-Specific Peptidase 10 (USP10) Inhibits Hepatic Steatosis, Insulin Resistance, and Inflammation Through Sirt6. *Hepatology (Baltimore, Md).* 2018;68:1786–1803.
65. Zhang C, Zhao H, Cai Y, Xiong J, Mohan A, Lou D, Shi H, Zhang Y, Long X, Wang J and Yan C. Cyclic nucleotide phosphodiesterase 1C contributes to abdominal aortic aneurysm. *Proceedings of the National Academy of Sciences of the United States of America.* 2021;118.
66. Goodwin LO, Splinter E, Davis TL, Urban R, He H, Braun RE, Chesler EJ, Kumar V, van Min M, Ndikum J, Philip VM, Reinholdt LG, Svenson K, White JK, Sasner M, Lutz C and Murray SA. Large-scale discovery of mouse transgenic integration sites reveals frequent structural variation and insertional mutagenesis. *Genome research.* 2019;29:494–505. [PubMed: 30659012]
67. Allahverdian S, Chaabane C, Boukais K, Francis GA, Bochaton-Piallat M-L. Smooth muscle cell fate and plasticity in atherosclerosis. *Cardiovasc Res.* 2018;114:540–550. [PubMed: 29385543]
68. Fanucchi S, Fok ET, Dalla E, Shibayama Y, Borner K, Chang EY, Stoychev S, Imakaev M, Grimm D, Wang KC, Li G, Sung WK and Mhlanga MM. Immune genes are primed for robust transcription by proximal long noncoding RNAs located in nuclear compartments. *Nat Genet.* 2019;51:138–150. [PubMed: 30531872]
69. Liu B, Sun L, Liu Q, Gong C, Yao Y, Lv X, Lin L, Yao H, Su F, Li D, Zeng M and Song E. A cytoplasmic NF- $\kappa$ B interacting long noncoding RNA blocks I $\kappa$ B phosphorylation and suppresses breast cancer metastasis. *Cancer Cell.* 2015;27:370–81. [PubMed: 25759022]
70. Mineo M, Lyons SM, Zdioruk M, von Spreckelsen N, Ferrer-Luna R, Ito H, Alayo QA, Kharel P, Giantini Larsen A, Fan WY, Auduong S, Grauwet K, Passaro C, Khalsa JK, Shah K, Reardon DA, Ligon KL, Beroukhim R, Nakashima H, Ivanov P, Anderson PJ, Lawler SE and Chiocca EA. Tumor Interferon Signaling Is Regulated by a lncRNA INCR1 Transcribed from the PD-L1 Locus. *Molecular cell.* 2020;78:1207–1223.e8. [PubMed: 32504554]
71. Agarwal S, Vierbuchen T, Ghosh S, Chan J, Jiang Z, Kandasamy RK, Ricci E and Fitzgerald KA. The long non-coding RNA LUCAT1 is a negative feedback regulator of interferon responses in humans. *Nat Commun.* 2020;11:6348. [PubMed: 33311506]
72. Caramori G, Adcock IM, Di Stefano A and Chung KF. Cytokine inhibition in the treatment of COPD. *Int J Chron Obstruct Pulmon Dis.* 2014;9:397–412. [PubMed: 24812504]

73. Ning Y and Lenz HJ. Targeting IL-8 in colorectal cancer. *Expert Opin Ther Targets*. 2012;16:491–7. [PubMed: 22494524]
74. Lane BR, Lore K, Bock PJ, Andersson J, Coffey MJ, Strieter RM and Markovitz DM. Interleukin-8 stimulates human immunodeficiency virus type 1 replication and is a potential new target for antiretroviral therapy. *Journal of virology*. 2001;75:8195–202. [PubMed: 11483765]
75. Stemmler S, Arinir U, Klein W, Rohde G, Hoffjan S, Wirkus N, Reinitz-Rademacher K, Bufe A, Schultze-Werninghaus G and Epplen JT. Association of interleukin-8 receptor alpha polymorphisms with chronic obstructive pulmonary disease and asthma. *Genes Immun*. 2005;6:225–30. [PubMed: 15772681]
76. Ha H, Debnath B and Neamati N. Role of the CXCL8-CXCR1/2 Axis in Cancer and Inflammatory Diseases. *Theranostics*. 2017;7:1543–1588. [PubMed: 28529637]
77. Bilusic M, Heery CR, Collins JM, Donahue RN, Palena C, Madan RA, Karzai F, Marté JL, Strauss J, Gatti-Mays ME, Schlom J and Gulley JL. Phase I trial of HuMax-IL8 (BMS-986253), an anti-IL-8 monoclonal antibody, in patients with metastatic or unresectable solid tumors. *J Immunother Cancer*. 2019;7:240. [PubMed: 31488216]
78. Hoffmann E, Dittrich-Breiholz O, Holtmann H and Kracht M. Multiple control of interleukin-8 gene expression. *Journal of leukocyte biology*. 2002;72:847–55. [PubMed: 12429706]
79. Bennett M, Ulitsky I, Alloza I, Vandenbroeck K, Miscianinov V, Mahmoud AD, Ballantyne M, Rodor J and Baker AH. Novel Transcript Discovery Expands the Repertoire of Pathologically-Associated, Long Non-Coding RNAs in Vascular Smooth Muscle Cells. *Int J Mol Sci*. 2021;22. [PubMed: 35008458]
80. Asfaha S, Dubeykovskiy AN, Tomita H, Yang X, Stokes S, Shibata W, Friedman RA, Ariyama H, Dubeykovskaya ZA, Muthupalani S, Ericksen R, Frucht H, Fox JG and Wang TC. Mice that express human interleukin-8 have increased mobilization of immature myeloid cells, which exacerbates inflammation and accelerates colon carcinogenesis. *Gastroenterology*. 2013;144:155–66. [PubMed: 23041326]
81. Posern G and Treisman R. Actin' together: serum response factor, its cofactors and the link to signal transduction. *Trends Cell Biol*. 2006;16:588–96. [PubMed: 17035020]
82. Cheng X, Yang Y, Fan Z, Yu L, Bai H, Zhou B, Wu X, Xu H, Fang M, Shen A, Chen Q and Xu Y. MKL1 potentiates lung cancer cell migration and invasion by epigenetically activating MMP9 transcription. *Oncogene*. 2015;34:5570–81. [PubMed: 25746000]
83. Xu H, Wu X, Qin H, Tian W, Chen J, Sun L, Fang M and Xu Y. Myocardin-Related Transcription Factor A Epigenetically Regulates Renal Fibrosis in Diabetic Nephropathy. *Journal of the American Society of Nephrology : JASN*. 2015;26:1648–60. [PubMed: 25349198]

## Clinical Perspective

### What is New?

- *INKILN* is a novel human-specific long noncoding RNA (lncRNA), which is downregulated in contractile vascular smooth muscle cells (VSMCs) and induced in human atherosclerosis and abdominal aortic aneurysm.
- *INKILN* promotes a proinflammatory VSMC phenotype and exacerbates injury-induced neointimal formation, which involves *INKILN* physical interaction with MKL1 and a deubiquitinase, USP10, to prevent ubiquitin-dependent MKL1 degradation.
- Bacterial Artificial Chromosome (BAC) transgenic mice offer an innovative, physiologically relevant approach to study the in vivo regulation and function of human-specific lncRNAs in models of human disease.

### What Are the Clinical Implications?

- Our findings provide new insight into therapeutic strategies for vascular disease via targeting the interplay between coding and noncoding pathways.
- Targeting *INKILN* gene expression represents a promising approach to control VSMC inflammation and vascular diseases.

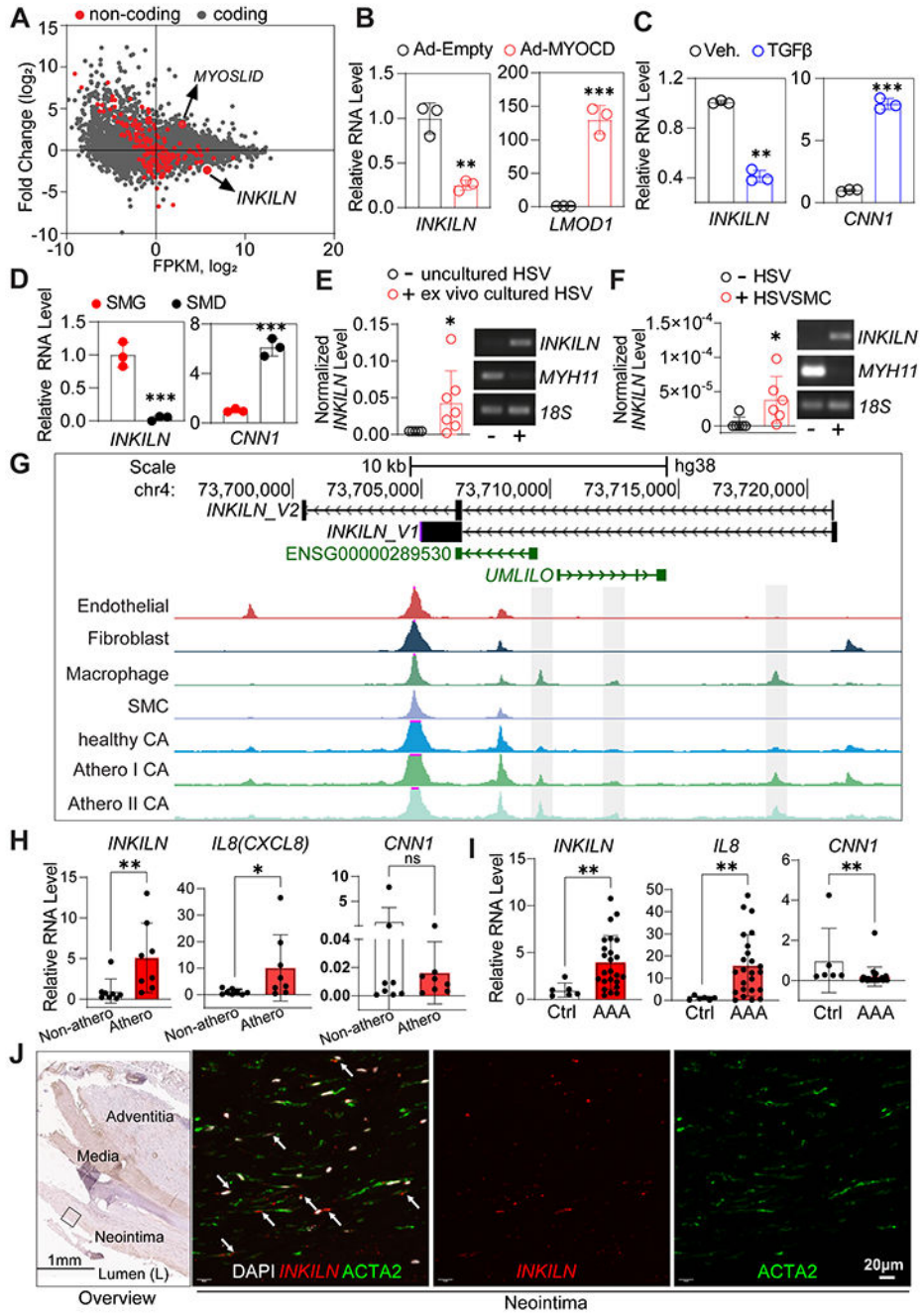


**Figure 1. *INKILN* expression correlates with VSMC phenotypic modulation and vascular disease.**

**A.** RNA-seq analysis revealed numerous coding (Gray dots) and noncoding genes (red dots) regulated by MYOCD in human coronary artery smooth muscle cells (HCASMCs) (n=2). **B-D.** qRT-PCR validation of the downregulation of *INKILN* in HCASMCs transduced with Ad-MYOCD relative to Ad-empty (**B**, n=3), differentiated HCASMCs induced by either TGFβ (2 ng/ml) (**C**, n=3) or conditioned SMC differentiation medium (SMD) versus growth medium (SMG) (**D**, n=3). **E.** qRT-PCR (left) and semi-qRT-PCR (right) analysis of the



indicated genes in uncultured versus 2 weeks ex vivo cultured human saphenous vein (HSV) segments from the same patients (n=7 patients). **F.** qRT-PCR (left) and semi-qRT-PCR (right) analysis of the indicated genes in uncultured HSV versus primary cultured SMCs dispersed from fresh HSV tissues (HSVSMCs) (n=6). **G.** UCSC genome browser screenshot of the *INKILN* gene locus with combined single nucleus (sn) ATAC-seq libraries from healthy versus diseased coronary artery (CA) human samples (n=41). Healthy CA: patient has no evidence of atherosclerosis and samples are lesion-free; Athero I CA: patient has evidence of atherosclerosis, but samples are lesion-free; Atherosclerosis II CA: patient has evidence of atherosclerosis and sample contains lesion. **H** and **I.** qRT-PCR assessment of the indicated genes in human atherosclerotic plaque (Athero) versus non-plaque (Non-athero) regions from the same patients (**H**, n=8 patients), and abdominal aortic aneurysm (AAA) tissues (n=24 patients) relative to healthy control aortas (Control) from organ donors (**H**, n=6 donors). **J.** Representative images of the overview for the colorimetric ACTA2 (brown) immunohistochemistry staining of human AAA tissues and Immuno-RNA FISH for *INKILN* (Red) and a VSMC marker ACTA2 (Green) in the rectangle marked neointimal region (see overview) of human AAA vessels (n=5 patients). Arrows indicate specific *INKILN* signal. **B-D**, and **F**, unpaired t-test; **E**, paired t-test; **H** and **I**, Mann-Whitney test. \*p<0.05, \*\* p <0.01, \*\*\* p <0.0001, ns, not significant.

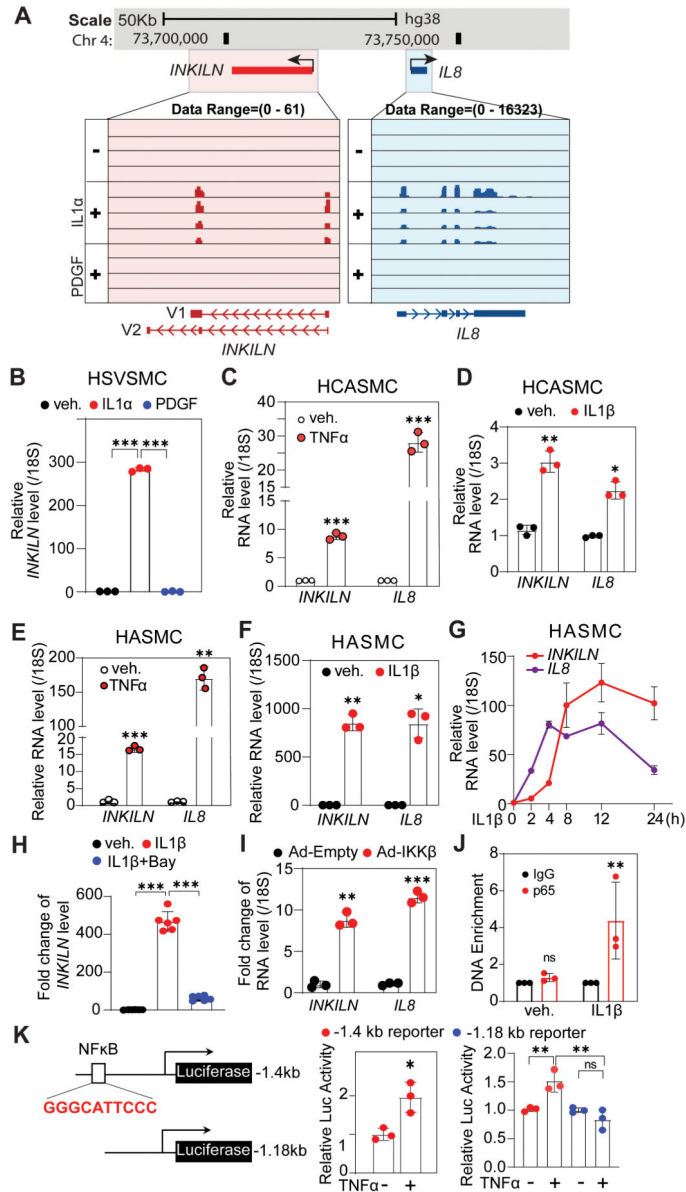


**Figure 2. *INKILN* is induced by proinflammatory stimuli through the NF-κB/p65-dependent pathway.**

**A.** *INKILN* and its neighboring gene *CXCL8 (IL8)* expression in primary HSVSMCs ± IL1α and PDGF mined from the RNA-seq dataset we published.<sup>54</sup> **B.** qRT-PCR analysis of *INKILN* expression in HSVSMCs induced with IL1α (10 ng/ml) and PDGF (20 ng/ml) relative to vehicle control (n=3). **C-F.** qRT-PCR assay for the indicated genes in HCASMCs ± TNFα (10 ng/ml) for 48 hours (**C**), HCASMCs ± IL1β (4 ng/ml) (**D**), human aortic SMCs (HASMCs) ± TNFα (10 ng/ml) (**E**) or IL1β (4 ng/ml) (**F**) for 24 hours (n=3). **G.** qRT-PCR for *INKILN* expression in HASMCs stimulated by IL1β (4 ng/ml) for the indicated time points (n=3). **H.** HASMCs were induced with IL1β (4 ng/ml) for 24 hours followed by treatment with BAY11-7082 (10 μM) for 24 hours before RNA extraction for qRT-PCR of the indicated genes (n=6). **I.** qRT-PCR analysis of *INKILN* in HASMCs transduced with

Ad-IKK $\beta$  or vector control adenovirus (Ad-Empty) with the same dose (MOI=30) for 72 hours (n=3). **J**. Chromatin Immunoprecipitation (ChIP)-qPCR validation of p65 binding to the predicted NF- $\kappa$ B site within the proximal *INKILN* promoter in HASMs induced by IL1 $\beta$  or vehicle control for 15 minutes (n=3). **K**. Schematic of luciferase reporter of the putative -1.4 kb *INKILN* proximal promoter containing a predicted NF- $\kappa$ B site and the truncated -1.18 kb reporter lacking this site, and luciferase assays for the -1.4 kb promoter of *INKILN* and the truncated reporter in HEK293 cells induced by TNF $\alpha$  (10 ng/ml) for 6 hours (n=3). **B**, one-way ANOVA followed by a Bonferroni test; **C-F, I, K** (left), unpaired t-test; **H**, Brown-Forsythe and Welch ANOVA test followed by Dunnett's multiple comparison test; **J**, and **K**(right), two-way ANOVA followed by a Tukey's post hoc test. \* p <0.05, \*\* p<0.01, \*\*\* p<0.0001, ns, not significant.

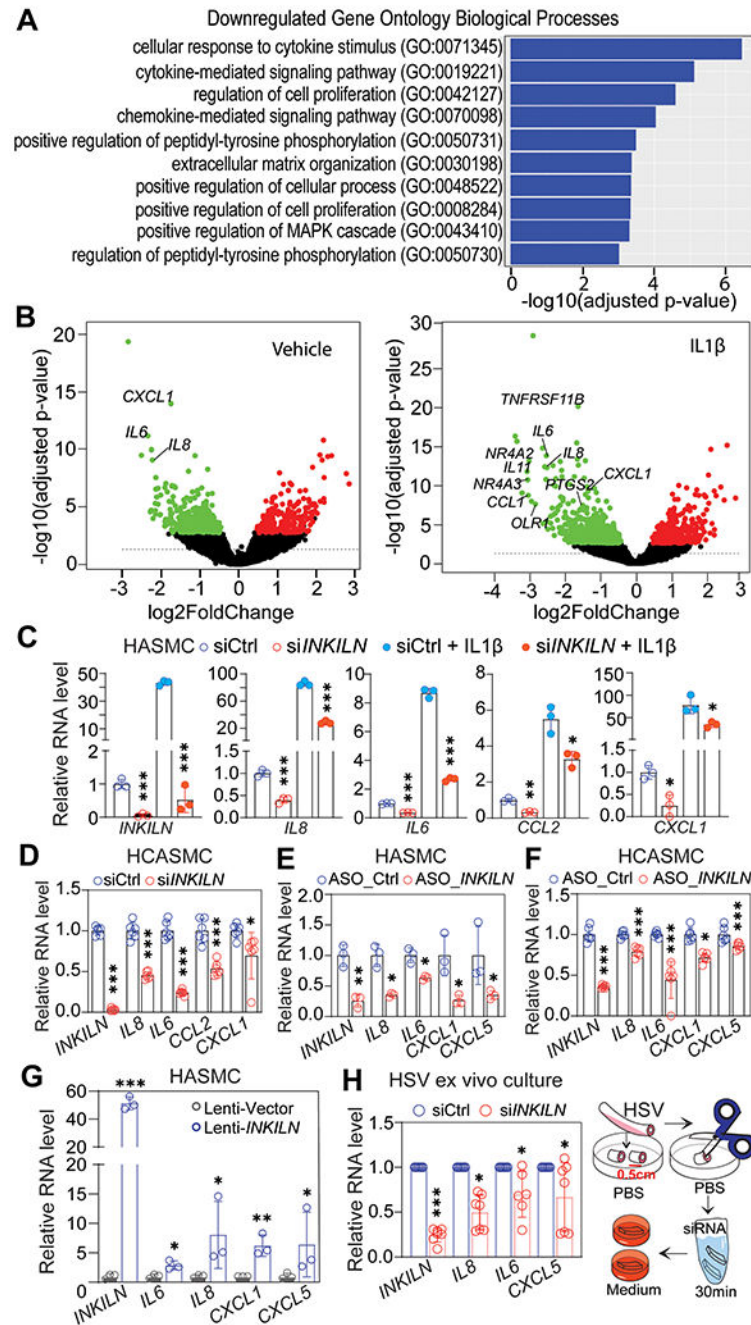


**Figure 3. *INKILN* positively regulates proinflammatory gene expression.**

**A.** The top 10 enriched Gene Ontology (GO) biological process terms downregulated by *siINKILN* in HASMCs under the IL1β-induced condition are shown (false discovery rate (FDR) adjusted p<0.05 and absolute log2FoldChange). Individual GO terms were sorted by adjusted p values. **B.** Volcano plot depicts the differentially expressed genes in HASMCs ± IL1β treated with *siINKILN* versus siCtrl (sicontrol). **C-F.** qRT-PCR validation of the reduced expression of the indicated pro-inflammatory genes upon *INKILN* depletion in HASMCs ± IL1β (**C**, n=3) and growing HCASMCs (**D**, n=6) using *siINKILN* versus siCtrl

(n=3) or FANA Antisense Oligonucleotides (ASO) to *INKILN* (ASO\_ *INKILN*) versus ASO control (ASO\_Ctrl) in growing HASMCs (**E**, n=3) and HCASMCs (**F**, n=3). **G**. Growing HASMCs transduced with the same amount of lentivirus carrying the *INKILN* (Lenti-*INKILN*) or lentivirus negative control (Lenti-vector) for 72 hours before RNA extraction for qRT-PCR of the indicated proinflammatory genes (n=3). **H**. HSV segments incubated with si*INKILN* or siCtrl for 30 minutes at the dose of 25 nM followed by ex vivo culture for 3 days before total RNA isolation for qRT-PCR of the indicated genes (each dot represents the average value from 3 separate segments from the same patient, n=6 patients). **C-G**, unpaired t-test; **H**, paired t-test. \* p<0.05, \*\* p<0.01, \*\*\* p<0.0001, ns, not significant.



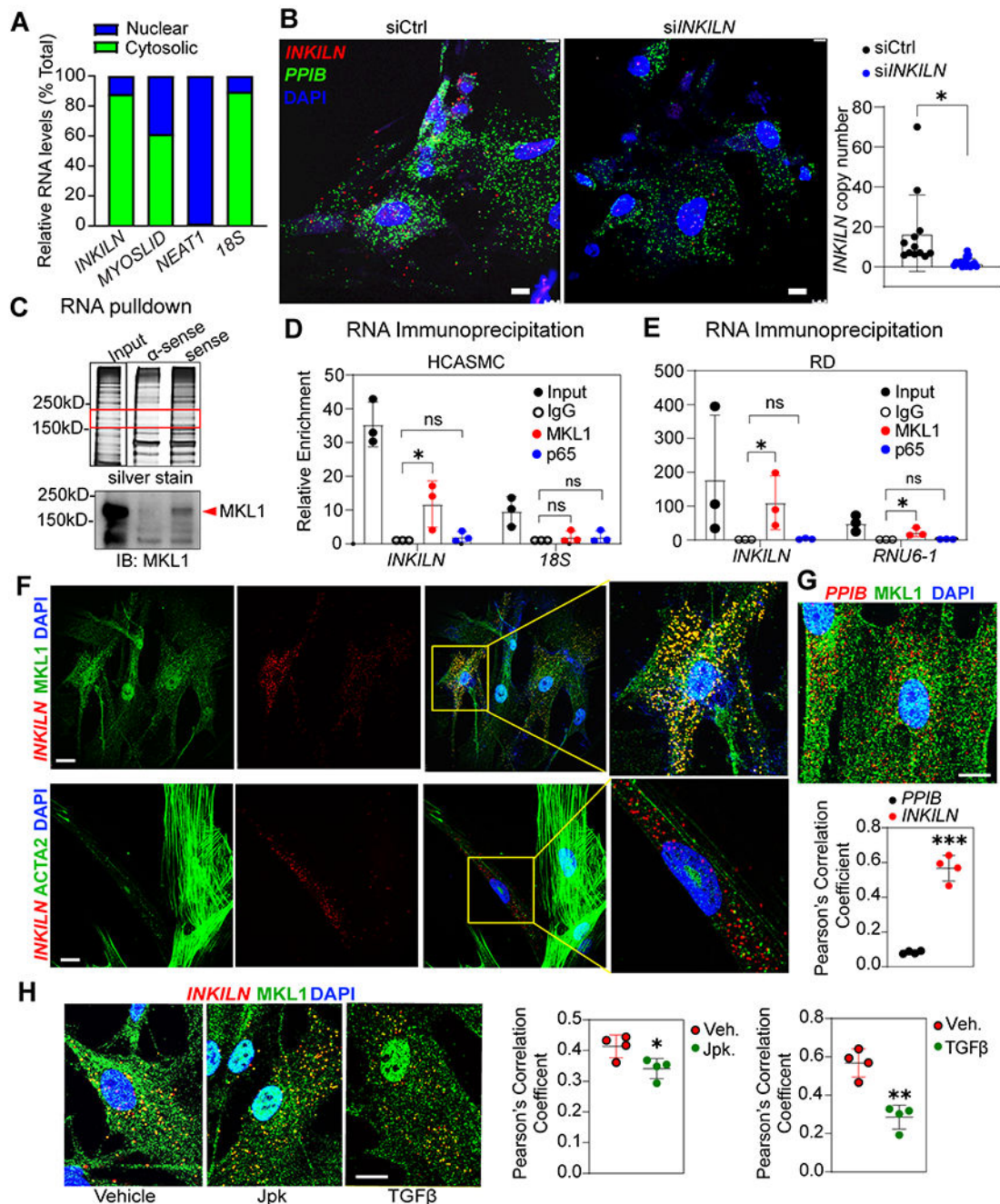


**Figure 4. *INKILN* interacts with *MKL1* in the cytoplasm of VSMCs.**

**A.** Representative qRT-PCR analysis of *INKILN* and the indicated control genes in total RNA from the fractionated cytosolic and nuclear compartments in HCASMCs (n=3 independent experiments). **B.** RNA-FISH for *INKILN* (red) and *PPIB* (green) and DAPI (blue) staining in growing HCASMCs and the quantitation of the copy number of *INKILN* per cell (n=12 fields with 39 cells for siCtrl and n=17 fields with 71 cells for siINKILN from 3 biological replicates quantitated). **C.** In vitro RNA pulldown using biotinylated sense *INKILN* and antisense *INKILN* RNA showed an enriched band between 150kD and 250kD

with sense *INKILN* by silver staining (red rectangle), which was validated as MKL1 protein by western blot (below). Representative images shown (n=3). **D-E**. Representative RNA Immunoprecipitation (RIP)-qPCR in HCASMC (**D**) and human rhabdomyosarcoma (RD) cells (**E**) showed an enrichment of *INKILN* from RNA precipitates by MKL1, but not p65 antibodies (n=3 independent experiments). **F-G**. Representative immuno-RNA-FISH for *INKILN* (red) and MKL1 protein (green) in HCASMCs (**F, G**) and the quantitation of the co-localization between *INKILN* and MKL1 protein by Pearson correlation coefficient analysis (**G**). *PPIB* mRNA was used as a negative control which fails to co-localize with MKL1 protein (quantitation was from 4 cells of 1 representative experiment out of 3 independent experiments). **H**. Representative immuno-RNA-FISH for *INKILN* and MKL1 protein in HCASMCs treated with Jaspilakinolide (Jpk) for 6 hours or TGF $\beta$  for 24 hours to induce MKL1 nuclear translocation, and the quantitation of the co-localization of *INKILN* with MKL1 by Pearson correlation coefficient analysis under both stimulation conditions relative to their individual vehicle controls (quantitation was from 4 cells of 1 representative experiment out of 3 independent experiments). Scale Bar =20 $\mu$ m. **B, G, and H**, unpaired t-test; **D** and **E**, one-way ANOVA followed by a Dunnett's test. \* p<0.05, \*\* p<0.01, \*\*\* p<0.0001, ns, not significant.

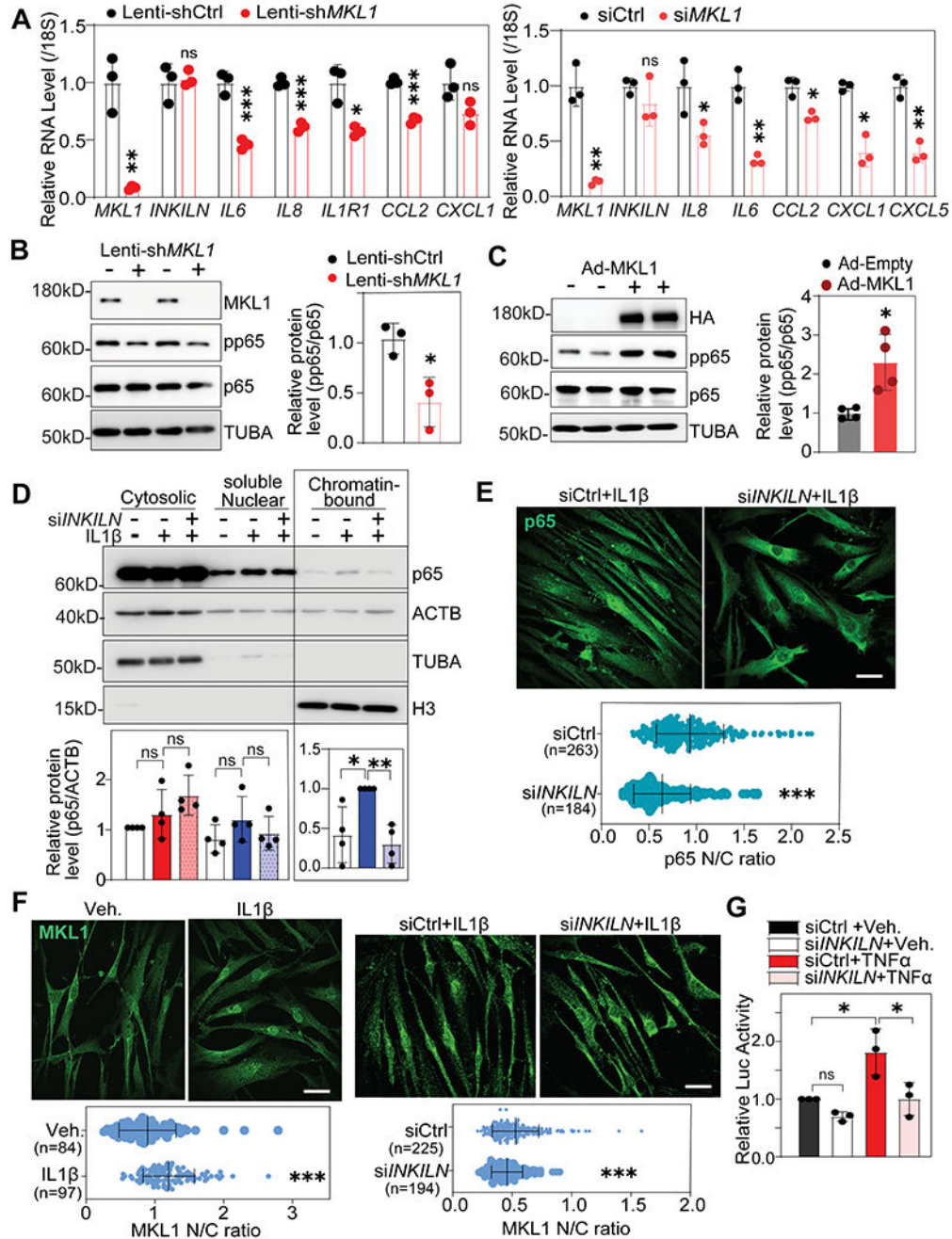


**Figure 5. Loss of *INKILN* suppresses MKL1/p65-mediated activation of the proinflammatory gene program.**

**A.** qRT-PCR analysis of the expression levels of the indicated proinflammatory genes in HCASMCs treated with same amount of lentivirus carrying short hairpin RNA to MKL1 (Lenti-sh*MKL1*) or siRNA SMART POOL to MKL1 (si*MKL1*) versus their individual controls (Lenti-shCtrl or siCtrl) (n=3). **B-C.** Representative western blot of the phosphorylated p65 (pp65) level in HCASMCs transduced with Lenti-sh*MKL1* versus Lenti-shCtrl (**B**, n=3) or Adenovirus carrying MKL1 transcript (Ad-*MKL1*) versus Ad-

empty control (Ad-empty) for 48 hours before protein extraction for western blot of the indicated proteins (**C**, n=4) and the respective quantitation. **D**. Representative western blot of fractionated proteins from the indicated cellular compartments in HCASMCs depleted by si*INKILN* for 48 hours followed by IL1 $\beta$  stimulation for 24 hours and the quantitation (n=4). **E**. Representative immunofluorescence staining for p65 protein in HASMCs treated with si*INKILN* or siCtrl for 48 hours prior to IL1 $\beta$  induction for 24 hours and the quantitation (n=3). **F**. Immunofluorescence staining for MKL1 in HASMCs treated with si*INKILN* versus siCtrl for 48 hours followed by IL1 $\beta$  induction for 24 hours (n=3 with indicated total cell numbers). **G**. Luciferase assay for NF- $\kappa$ B reporter activity in HASMCs depleted by si*INKILN* for 48 hours followed by TNF $\alpha$  (10 ng/ml) stimulation for 6 hours (n=3). **A-C**, unpaired t-test; **D**, Brown-Forsythe and Welch ANOVA test followed by Dunnett's multiple comparison test; **E** and **F**, Mann Whitney test; **G**, two-way ANOVA followed by a Tukey's post hoc test. \* p<0.05, \*\* p<0.01, \*\*\* p<0.0001, ns, not significant.



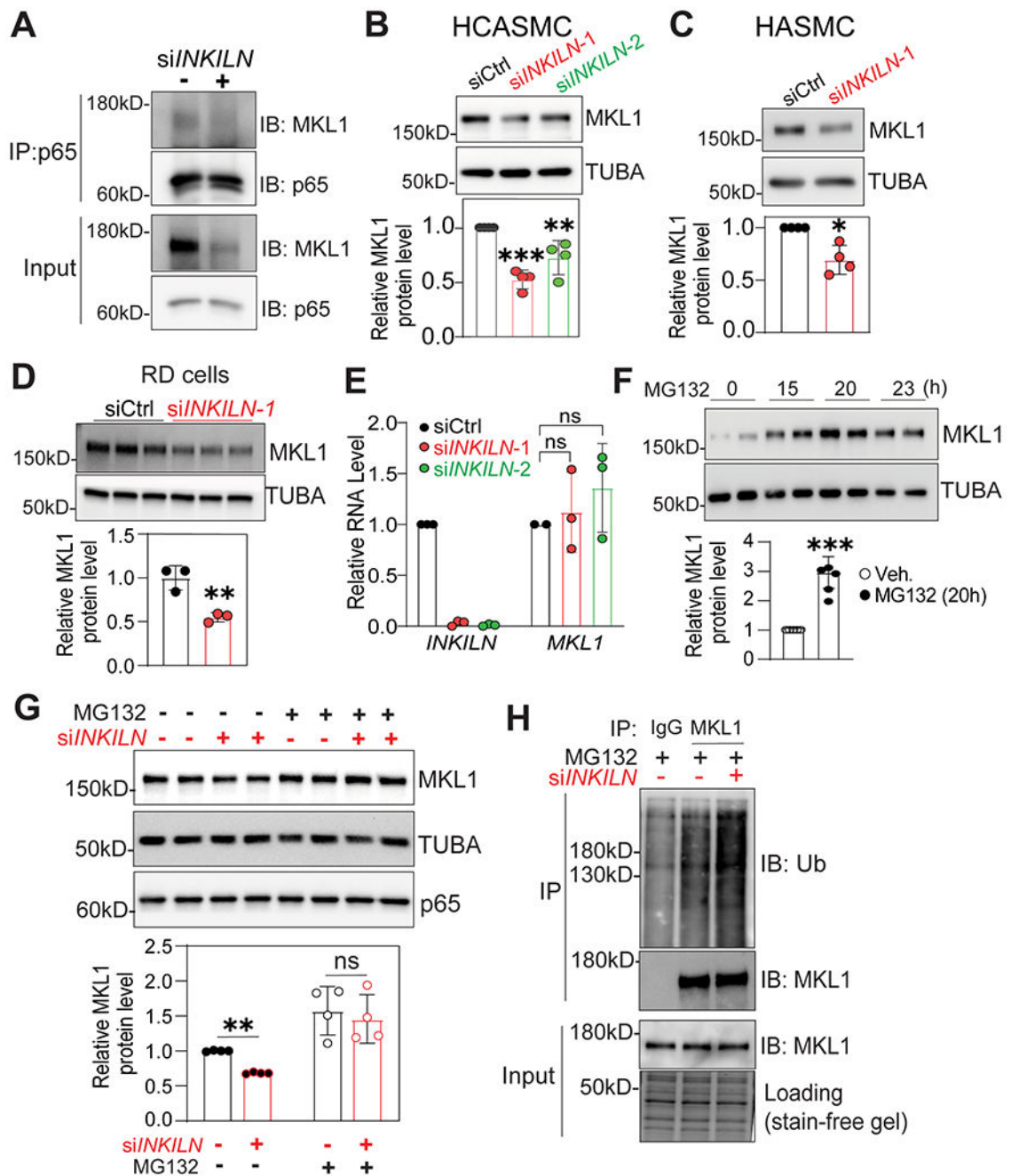


**Figure 6. Loss of *INKILN* reduces MKL1 protein stability via enhancing ubiquitination proteasome degradation.**

**A.** HASMCs were transfected with si*INKILN* or siCtrl for 48 hours prior to protein extraction for p65 immunoprecipitation followed by western blotting analysis of the indicated proteins. 1/100 amount of total cell lysates were used as input control. Representative western blot images for the indicated proteins (n=5). **B-D.** HCASMCs (**B**, n=4), HASMCs (**C**, n=4), and RD cells (**D**, n=3) were treated with si*INKILN* or siCtrl for 72 hours and protein lysates were used for western blot analysis of MKL1. Representative



western blot images (**B-D**, top) and the quantitation (**B-D**, bottom). **E**. qRT-PCR of *MKL1* mRNA expression after siRNA-mediated *INKILN* gene knockdown in HCASMCs (n=3). **F**. HASMCs treated with 5 $\mu$ M MG132 for the indicated time before protein extraction for western blot of MKL1. Representative western blot (top) and the quantitation at 20 hours after the treatment of MG132 (bottom) (n=5). **G**. HASMCs treated with siRNA for 48 hours followed by MG132 (5  $\mu$ M) for 20 hours prior to protein extraction for western blot of MKL1. Representative western blot image (top) and the quantification (bottom) (n=4). **H**. HCASMCs treated with si*INKILN* versus siCtrl for 48 hours followed by MG132 (5  $\mu$ M) treatment for 20 hours prior to protein extraction for immunoprecipitation of MKL1 and western blot of ubiquitin. Representative images shown (n=4). **B** and **E**, one-way ANOVA followed by a Bonferroni test; **C**, **D**, and **F**, unpaired t-test; **G**, two-way ANOVA followed by a Bonferroni test. \* p<0.05, \*\* p<0.01, \*\*\* p<0.0001, ns, not significant.

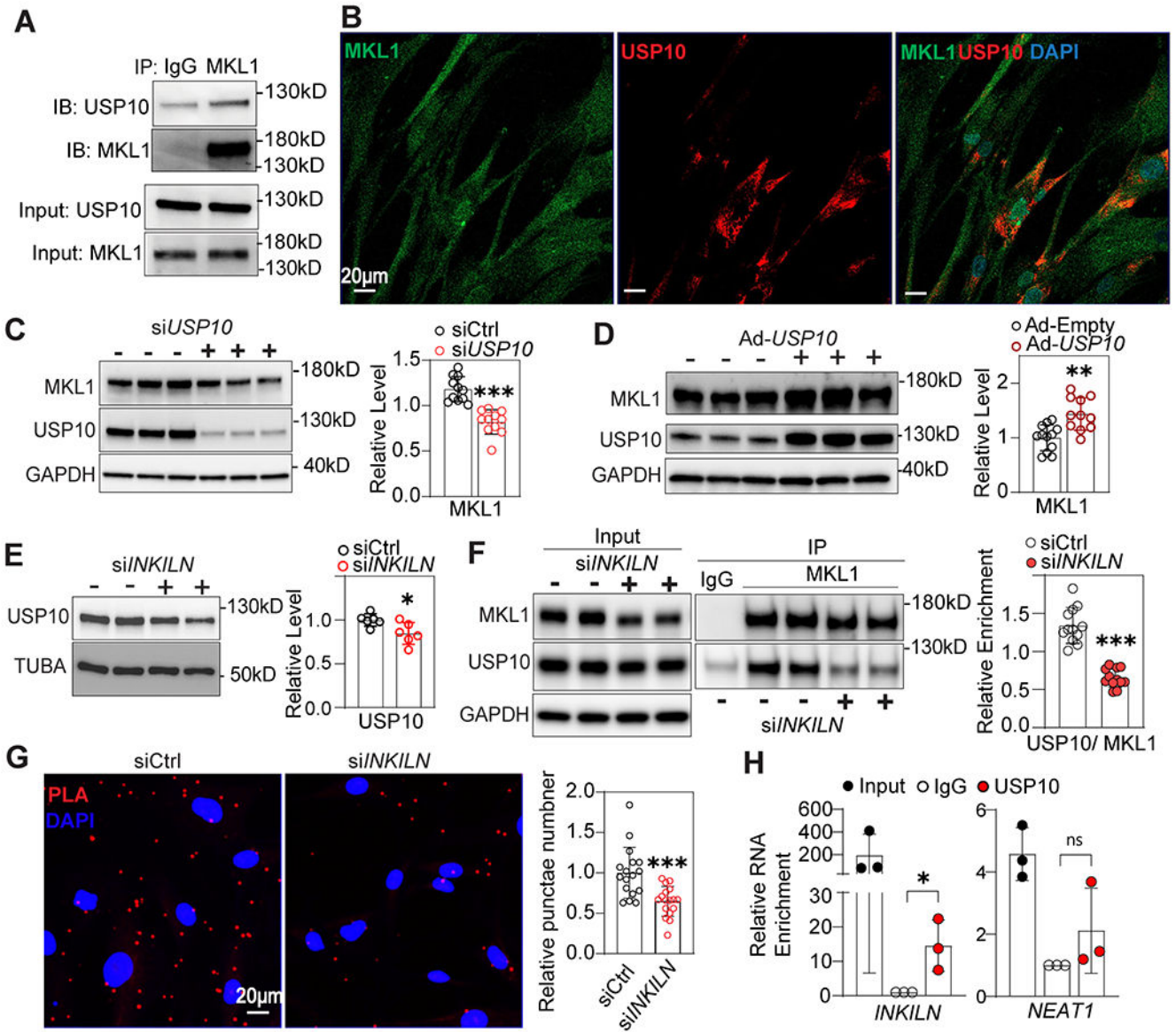


**Figure 7. *INKILN* facilitates the interaction between MKL1 and USP10.**

**A.** Representative image of co-immunoprecipitation of MKL1 followed by western blot of the indicated proteins in HCASMCs (n=4). **B.** Representative co-immunofluorescence staining of MKL1 and USP10 in HCASMCs (n=3). Scale Bar=20 $\mu$ m. **C,D.** Representative western blot of the indicated proteins in HCASMCs treated with siRNA to *USP10* (C), or adenovirus overexpressing *USP10* (D) versus their individual controls and the quantitation of MKL1 protein levels (n=11). **E.** HCASMCs were treated with siRNA-*INKILN* for 72 hours and the protein levels of USP10 were detected by western blot (n=6). **F.** HCASMCs were treated with siRNA-*INKILN* for 72 hours prior to immunoprecipitation of MKL1 and western blot of the indicated proteins. Representative image and the quantitation of 8 biological replicates from 4 independent experiments. **G.** Representative image of proximity ligation assay (PLA) for MKL1 and USP10 in HCASMCs, and quantitation of PLA punctae

shown (17 fields from n=5 independent experiments). **H.** qRT-PCR of the indicated genes from the RNA pools precipitated by USP10 antibody in HCASMCs (n=3). Unpaired t-test for all the comparisons. \* p<0.05, \*\* p<0.01, \*\*\* p<0.0001, ns, not significant.

Author Manuscript

Author Manuscript

Author Manuscript

Author Manuscript

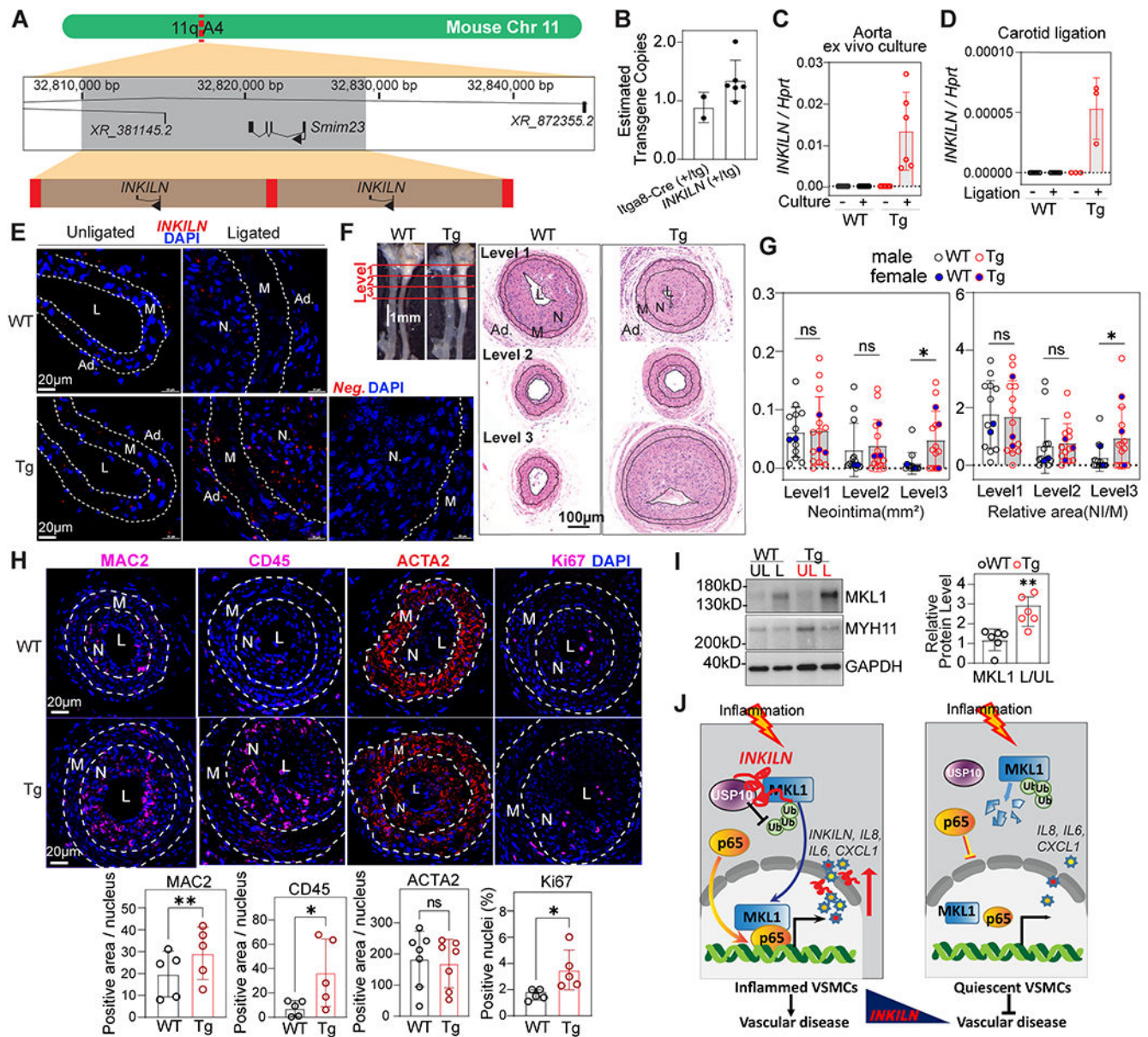


**Figure 8. *INKILN* expression in BAC transgenic mice and its influence on neointimal formation.**

**A.** CRISPR-LRS mapped a single integration locus for human *INKILN*. The integration locus, indicated by a grey box, spanned 32,808,215bp - 32,828,044bp on mouse chromosome 11 (mm10), disrupting testis-specific protein-coding gene, *Smim23*. *INKILN* BAC transgenes (brown rectangles), integrated in a tandem head to tail fashion accompanied with BAC cloning vector sequence (red boxes). **B.** qPCR determined ~2 transgene copies for human *INKILN*(+/tg, n=6) with data normalized to internal control locus. *Iiga8-CreER<sup>T2</sup>* mice (n=2) served as calibrator for one copy of a transgene.<sup>84</sup> Values graphed as mean ± SEM. **C.** qRT-PCR of *INKILN* for the uncultured versus 3 days ex vivo cultured aorta segments from WT and *INKILN*transgenic (Tg) mice (n=6). **D.** qRT-PCR of *INKILN* for unligated versus 1 week ligated carotid arteries from WT and Tg mice (n=3). **E.** Representative RNA FISH image for *INKILN*transcripts in unligated versus 4 week ligated

carotid arteries from WT and Tg mice (n=3). **F, G.** Representative whole mount of 4 week ligated carotid arteries from WT versus Tg mice (**F**, left), the H&E staining of sections at different levels (**F**, right), and the quantitation of neointimal formation (**G**, n=13 for WT and n=15 for Tg). Representative images of immunofluorescence staining (**H**) for the indicated proteins on cross sections of ligated carotid arteries from WT and Tg mice and the quantitation of the fluorescence positive area over the total nuclei at neointima and media (n= 5 mice, 1 section/mouse at level 3). **I.** Western blot of the indicated proteins in unligated and ligated carotid arteries from WT versus *INKILN*Tg mice and the quantitation (n=6). NI, Neointima; M, Media; UL, unligated carotids; L, ligated carotids. **G** and **I**, Mann-Whitney test; **H**, paired t-test. \*p<0.05, \*\*p<0.01, ns, not significant. **J.** Working model of *INKILN* activating VSMC inflammation. Inflammation induces *INKILN* expression, which inhibits MKL1 ubiquitin proteasome degradation via USP10 and enhances both MKL1 and p65 nuclear translocation, resulting in the increased nuclear interaction of MKL1 with p65 and subsequent transactivation of the proinflammatory gene program.